Department of Mechanical Engineering

Delhi Technological University
Delhi

CERTIFICATE

This is to certify that the thesis entitled **"Synthesis of Copper –Graphite Composite using Friction Stir Processing and evaluation of optimal parameters using Taguchi analysis"** submitted by **Anshul Jain(2K15/PIE/03)**, during the session 2015-2017 for the award of M.Tech degree of Delhi Technological University, Delhi is absolutely based upon his work done under my supervision and guidance and that neither this thesis nor any part of it has been submitted for any degree/diploma or any other academic award. The assistance and help received during the course of investigation have been fully acknowledged. He is a good student and I wish him good luck in future.

Mr.V Jeganathan Arulmoni
Associate Professor
Department of Mechanical Engineering
Delhi Technological University

Dr. RS Mishra
Head Of Department
Department of Mechanical Engineering
Delhi Technological University

ACKNOWLEDGEMENT

I like to express my deep sense of respect and gratitude to my project guide Mr. V.Jeganathan and Co-guide Dr. RS Mishra, Department of Mechanical Engineering, Delhi Technological University, Delhi for his invaluable and fruitful constructive suggestions and guidance that have enabled me to overcome all the problems and difficulties while carrying out multi-functionaries of the present investigation. I feel fortunate for the support, involvement and well wishes of my mentors and this is virtually impossible to express them in words. I also wish to express my gratitude to all the teachers and staff members of the Mechanical Engineering Department for their invaluable help throughout the course.

DECLARATION

I, **Anshul Jain**, hereby certify that the work which is being presented in this thesis entitled **"Synthesis of Copper –Graphite Composite using Friction Stir Processing and evaluation of optimal parameters using Taguchi analysis"**, is submitted, in the partial fulfillment of the requirements for degree of Master of Technology at Delhi Technological University is an authentic record of my own work carried under the supervision of **Mr. V Jeganathan Arulmoni & Dr. RS Mishra**. I have not submitted the matter embodied in this report for the award of any other degree or diploma also it has not been directly copied from any source without giving its proper reference.

Anshul Jain
2K15/PIE/03
M.Tech (Production Engineering)
Delhi Technological University

Abstract:

This report is concerned with the fabrication of surface composites. Surface composites are a group of modern engineered materials where the surface of the material is modified by dispersing secondary phase in the form of particles or fibers and the core of the material experience no change in chemical composition and structure. The potential applications of the surface composites can be found in automotive, aerospace, biomedical and power industries. Recently, friction stir processing (FSP) technique has been gaining wide popularity in producing surface composites in solid state itself. Friction Stir Processing (FSP) is a solid state surface composites producing process which uses a non-consumable rotating tool inserted into the workpiece for heating and softening the material. This results in material severe plastic deformation resulting in improved mechanical properties and refined grain structure. Most of the research conducted on FSP is confined to aluminum alloys; limited study is done on FSP of copper based alloys. Friction stir processing has been utilized to create metal matrix composites by consolidating graphite particles in a copper material matrix. Mechanical properties (i.e. tensile and hardness/microhardness, wear resistance etc.) of the matrix metal matrix composites reinforced with graphite particles. Tensile tests exhibited decrements in yield strength. The average microhardness value within the stir zone decreased from 180 HV in the base material to a minimum of 142HV in a graphite reinforced composites. Wear resistance is enhanced with decrease in the friction coefficient from 0.490 of standard specimen to minimum of 0.168.

CONTENTS

LIST OF TABLES

LIST OF FIGURES

LIST OF FIGURES

CHAPTER-1

INTRODUCTION

1.1Background:

At first, FSP was utilized for microstructural refinement of aluminum and magnesium combinations. FSP advancement has facilitated led to the fruitful handling of composites of copper, titanium and steel. FSP has likewise exhibited its effectiveness in homogenizing powder metallurgy handled aluminum combinations, microstructural modification of metal framework composites. FSP adequately eliminates throwing abandons, separates or dissolves second stage particles and prompt the extensive improvement in properties [23].

FSP has definite advantages compared to other metalwork methods. To start with, FSP is an immediate strong state preparing method that achieves microstructural change, densification, and homogeneity at the same time. Second, by rewriting the tool design, FSP parameters, and dynamic cooling/heating the microstructure and mechanical properties of the handled zone can be decisively overseen. Third, the depth of the processed zone can be optionally controlled by altering the length of the tool pin. Fourth, having a broad capacity for the manufacture, handling, and amalgamation of materials FSP is a versatile strategy. Fifth, FSP is a green and vitality effective method without hurtful gas, radiation, and commotion since the warmth contribution amid FSP originates from grinding and plastic twisting. 6th, FSP does not modify the shape and size of the processed specimens [24].

Though FSP was initially employed for microstructural refinement of aluminum and magnesium alloys, it is a very attractive process for also fabricating composites. Mishra et al. [8] fabricated the SiC/Al surface composites by FSP, and indicated that SiC particles were well distributed in the Al matrix, and good bonding with the Al matrix was generated. There are numerous conventional methods for fabricating surface composites such as powder metallurgy, laser melt treatment, plasma spraying, stir casting etc but these techniques lead to the deterioration of composite properties due to interfacial reaction between reinforcement and the metal matrix [10]. FSW/FSP may also be called as Green Technology as these processes will not pollute the environment[2]. These techniques involve the material transformation from solid to liquid or vapour state during the process as compared to solid state processing technique. Moreover, precise control of processing parameters is required to obtain desired microstructure in surface layer after solidification. FSP is one of the solid state processing techniques which have proved its potential in fabrication of all variants of surface composites with little or no interfacial reaction with the reinforcement. The potential applications of the surface composites can be found in automobile, aerospace, marine and power generation industries. Despite considerable interests in the FSP technology in past decade, the basic physical understanding of the process is lacking. Some important aspects, including material flow, tool geometry design, wear of welding tool, micro structural stability, welding of dissimilar alloys and metals[1].

In the most recent decade, investigated the potential of FSP procedure in manufacturing graphite strengthened surface composite layer on copper combination. From that point forward, a variety of surface composites in light of magnesium, copper, titanium and steel have been produced. In any case, far reaching

coverage of surface composites arranged by FSP is exceptionally constrained [24]. The present thesis is centered around the synthesis of copper graphite composite through friction stir processing and determining optimal processing parameters using Taguchi analysis.

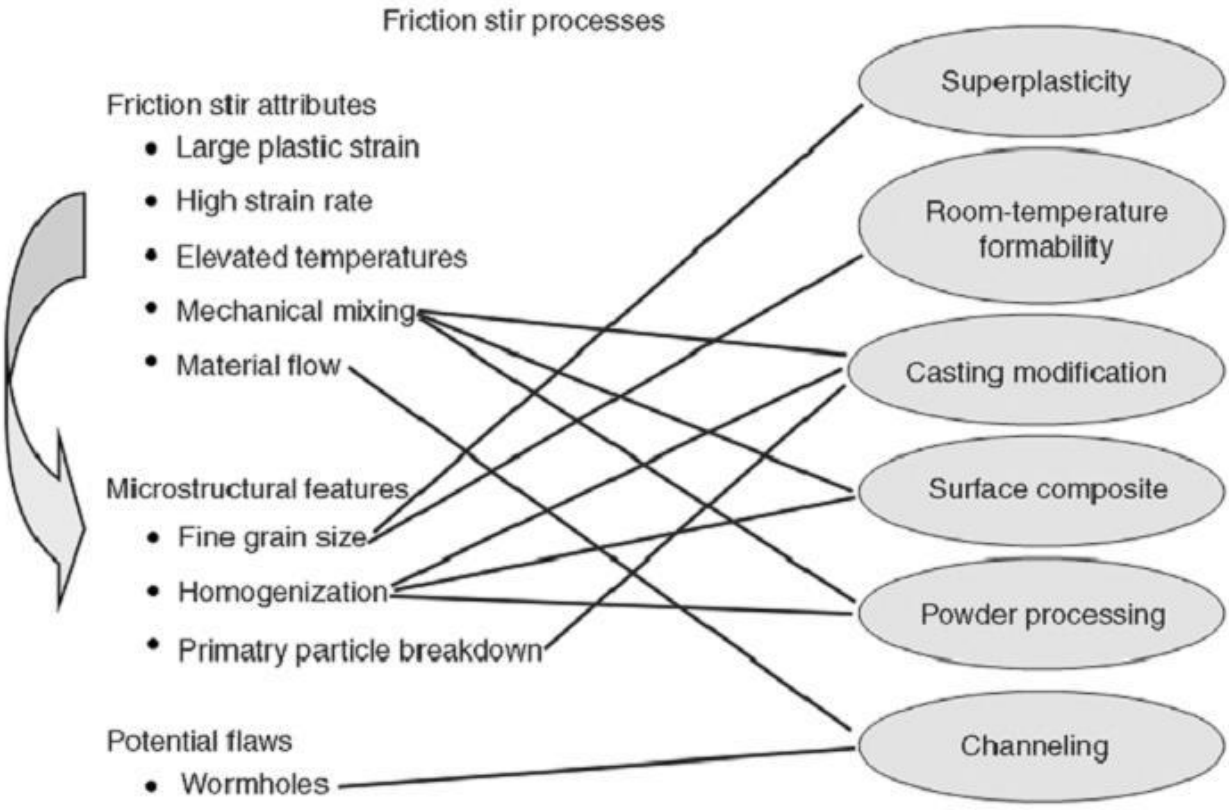

Figure 1.1 Schematic view of list of attributes and links to the FSP processes [26]

1.2 FSP Material:

Copper and its alloys are broadly utilized as material for a few parts in electrical, thermal, substance, atomic and transportation ventures. They show great mix of electrical conductivity, thermal conductivity and workability. Enhanced wear resistance what's more, arcing resistance of copper are required in applications, for example, electrical contacts, nozzles and bushes for bearings [25]. Copper is generally utilized as a part of optical and electronic businesses in light of its high electrical, high thermal conductivity and great corrosion resistance. Be that as it may, in pure form it has poor quality, wear also, fatigue resistance and consequently is inadmissible for applications requesting high fatigue and wear resistance like contact terminals of electrical switches [26].

1.3. Friction Stir Processing tool design:

As a result of the different geometrical elements of the tools the material movement around the tool pin is particularly mind boggling and significantly dissimilar from one tool to the other. Accordingly, the FSP tools can be categorized in three groups as shown in Figure 1. The fixed pin tool is a singular piece including the pin and shoulder (Figure 1a). Having an invariable pin length, this type of tool is suitable to process a workpiece with a constant thickness. The adjustable tool includes two pieces, which shoulder and pin move independently, to allow tuning of the pin length during FSP (Figure 1.2b) [29]. The shoulder and pin, in this design, can be fabricated employing different materials. Also, the worn or broken probe can be simply substituted. Moreover, using an adjustable tool, it is possible to process inconsistent and multiple gauge thickness workpieces. Also, the key hole remains at the end of the friction stir processing seam can be easily filled by using an adjustable tool [30]. The bobbin type tool (Figure 1.2c) includes three pieces which is shown in the figure 2. The movable pin length within top and bottom shoulders, in this type of tool, allows it to covers multiple gauge thicknesses.

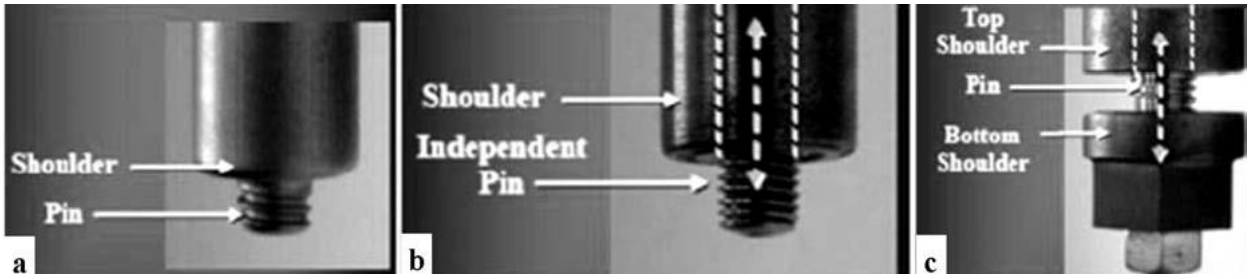

Figure 1.2: FSP different types of tools. a) fixed, b) adjustable, c) bobbin

1.4 Tool shapes

Tool shoulder components are basically designed to generate frictional heat and apply the required downward force to consolidate and maintain the soften metal underneath of shoulder surface. The standard outer surfaces of shoulder, the bottom and end surfaces features are summarized in Figure 2. Generally, the shoulder outer surface includes a cylindrical or conical profile. Since the shoulder plunge depth is usually small (1–5% of the gauge thickness) the influence of the shape of outer surface shoulder (cylindrical/conical) is believed to be minor.

Three varieties of shoulder end surfaces are illustrated in Figure 3. The most straightforward design is the flat shoulder end surface. This type of shoulder is not able to entrap the flowing material under the shoulder surface and causes the formation of unwarranted material flash. A inward curved(concave) shoulder end surface, be that as it may, is intended to limit the material expulsion from the edges of the shoulder [34]. Another practical end state of the shoulder is a convex curve profile [35]. When using a convex shoulder profile for joining to workpieces via friction stir welding, the major benefit is that the contact with the workpiece can be accomplished at any area down the end surface. In this manner, variety in levelness or

thickness between the two abutting edges. On the other hand, the failure to avoid material displacement away from pin leads to an unreliable weld using a convex shoulder profile [30].

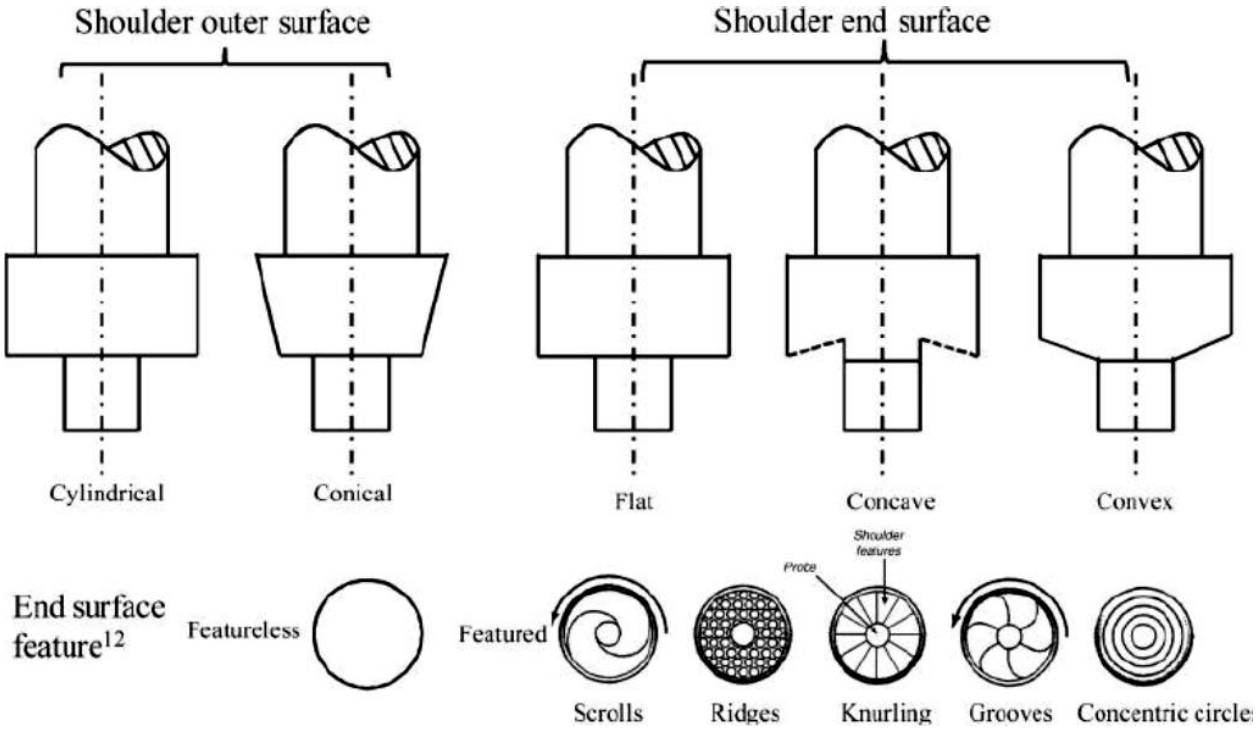

Figure 1.3: FSP tool shoulder shapes and features [36]

The Tool Pin is mainly responsible for distributing the contacting surface of workpiece, cut the metal in face of the tool and move the plasticized metal behind the tool. The depth of processed zone and maximum traverse speed are controlled by the pin geometry. As categorized in Figure 2, the tip of the pin can be either flat or round. Since the convenience of manufacturing a flat tip is greatest, it is the most commonly used geometry. This type of pin induces excessive forging force during the penetration phase. The domed tip shape, however, as result of lower forging force during the plunging, induces less tool wear leading to longer tooling life by eliminating locally developed stress concentration [30].

The FSP tool pin may have either a cylindrical surface or a tapered curved surface. A tapered pin, generally, has larger contact area with the workpiece leading to elevated frictional heat and increasing the plastic deformation. Although, causes severe tool wear, the tapered shape, also, induces a high hydro-static pressure in the process area which is particularly critical for enhancing the material mixing and processed zone uniformity.

Various shapes and features can be considered on the pin outer surface including threads, flats or flutes. For processing high strength or extremely abrasive alloys thread-less pins are better choices as these features could be easily worn away. However, the most common type of outer surface feature is the thread. In particular, a left hand thread pin given clockwise movement which produces a downward metal flow from

the threads along the front surface [37]. It is, also, been found that flat features on the pin surface, increasing the local plasticized zone and rigorous(turbulent)flow of the plasticized material, can alter metal material movement around the pin [16]. The main function of flats on the pin is analogous to the edge's cutter. The material (powder form) is enclosed in the prepared flats and help in relieving metal at the back of the pin, promoting efficient mixing.

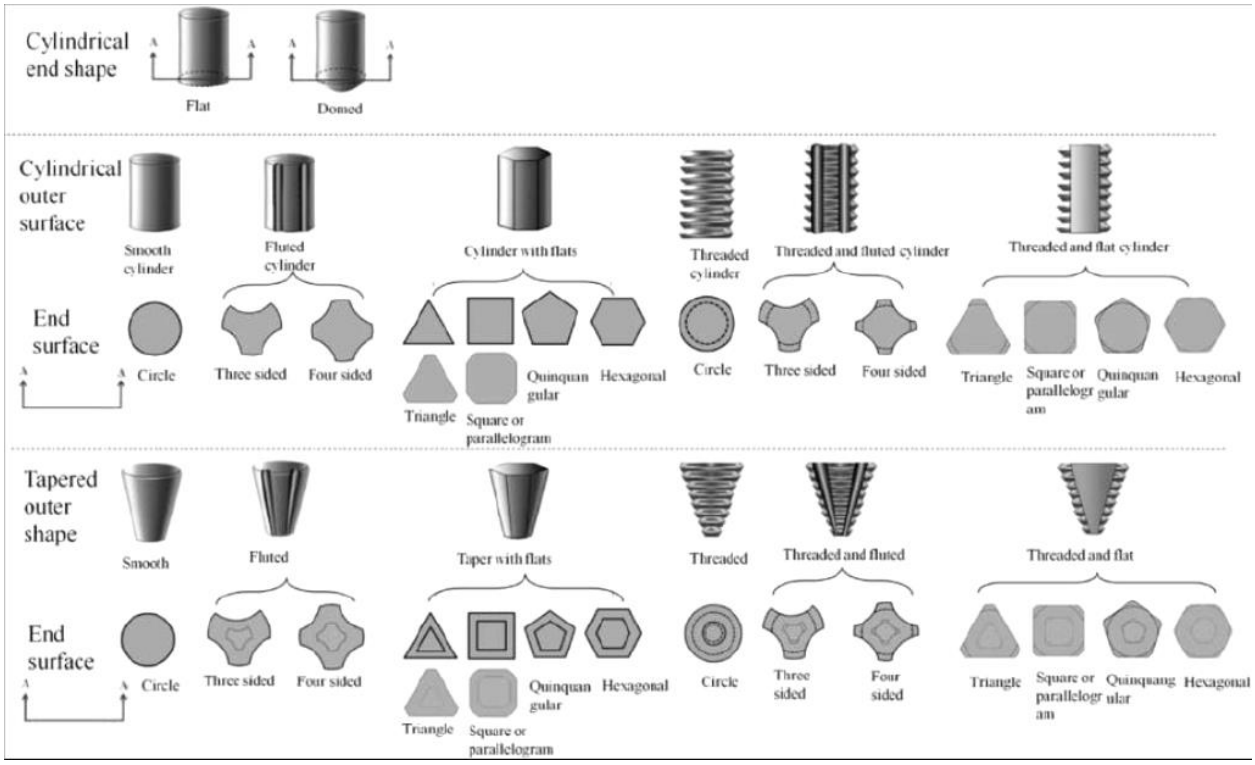

Figure1.4. FSP/FSW tool pin shapes [30]

1.5 Tool materials

The workpiece and the enhanced tool life are the two most crucial parameters to indicate the tool material. The following characteristics should be considered when selecting tool material:

- Superior compressive yield strength at high temperature than the predictable forging force onto tool.
- Dimensional stability and creep resistance
- High thermal fatigue strength to endure frequent heating and cooling cycles.
- Zero destructive reaction with the workpiece material.
- High fracture toughness to resist the forging force during penetration and dwelling.
- Minimum coefficient of thermal expansion difference between the pin and the shoulder to reduce the thermal stresses.
- Good machinability to facilitate cutting complex features on the tool.

1.6 Fabrication MMCs using FSP

It is all around recorded that the size and amount of reinforcement and in addition the attributes of metal matrix interface control the mechanical properties of MMCs[40]. Powder metallurgy (P/M) technique or liquid metal preparing have been the primary courses to manufacture solute(particle)-reinforced MMC's. Be that as it may, getting a uniform scattering of fine solute particles inside the matrix is particularly testing through conventional methods or P/M preparing. It is for the most part a result of the common pattern of fine particles to agglomeration amid mixing of the base material and the reinforced powders.
It has been demonstrated that FSP can be utilized to create copper matrix composites in-situ without supplementary combination prepare. The use of FSP to create MMCs has the accompanying points of interest[41]:

- Introducing separate plasticisity to mix and refine the constituent stages of phases in the material.
- Giving high temperature to facilitate the insitu response to create strengthening particles.
- Making hot consolidation build up a completely thick strong solid

.

Then again, the closeness of the reinforcing particles in the metallic matrix prompts reduced ductility which by and large is not attractive. Hence, rather than mass support, fuse of the particles to the surface improves the wear properties, which is a surface dependent reducing mode, without giving up the bulk properties[42]. Be that as it may, it is trying to successfully scatter particles on a metallic surface by ordinary surface treatments. The current preparing procedures to create surface composites depend on molten stage processing at lifted temperatures. Notwithstanding, it is hard to anticipate interfacial response amongst reinforcement and MMC and the production of some toxic process. Likewise, to accomplish consummate cemented microstructure in surface layer screen of handling parameter is by all accounts vital. Clearly, handling of surface composite at low temperature, underneath the melting point, can keep these issues [43]. For this situation, FSP, as a strong state handling strategy can be effectively utilized to create surface composites.

The primary trouble in manufacture of particulate composites is the agglomeration of fine reinforced particles. By effectively planning the tool specifications, which chiefly produces required frictional and shear strength, the inclination of solute agglomeration can be prominently directed. In addition, the oxide film encompassing reinforced particles can be broken because of extensive plastic strain in FSP, prompting significant contact between the reinforcement and matrix. As the measure of heat input assumes the key part in creating an imperfection free composite streamlining process parameters to produce appropriate measure of heat is basic to get a sound composite [37].

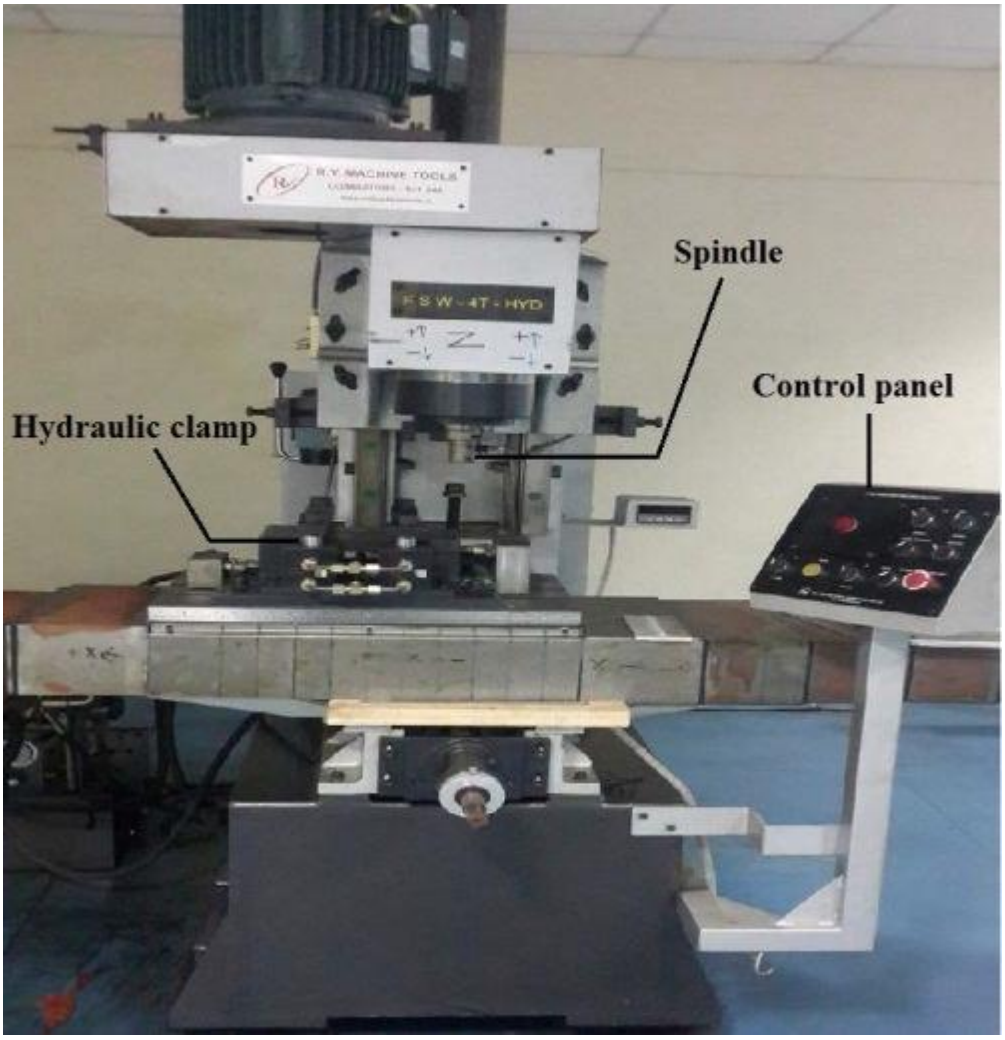

Figure1.5 Friction stir welding / processing machine (Central workshop, DTU)[22]

A clamping framework was composed keeping in mind the end goal to keep up the workpiece in position amid the procedure. Four mild steel pieces brace the workpiece on top with the goal that the substantial contact region makes enough drive to dodge any movement, the clamps were hydraulically operated.
In the present study, the production of composite through FSP is first performed by mixing the graphite powders in the copper matrix by machining a groove of 1 mm width and 2.5 mm inner depth in the plate to oblige the reinforcing. A cylindrical shape tool without pin was then used to entrap the material in the plate and close the upper surface of the groove by means of surface pressing (topping pass). In spite of the fact that, the topping pass keeps discharge of the particles from the groove amid the FSP, smooth thin copper layer made at topping pass mostly fills the section and pushes the particles toward the finish of the depression. In this manner, notwithstanding utilizing the topping pass the volume portion of the particles won't be the same as the underlying powder content.

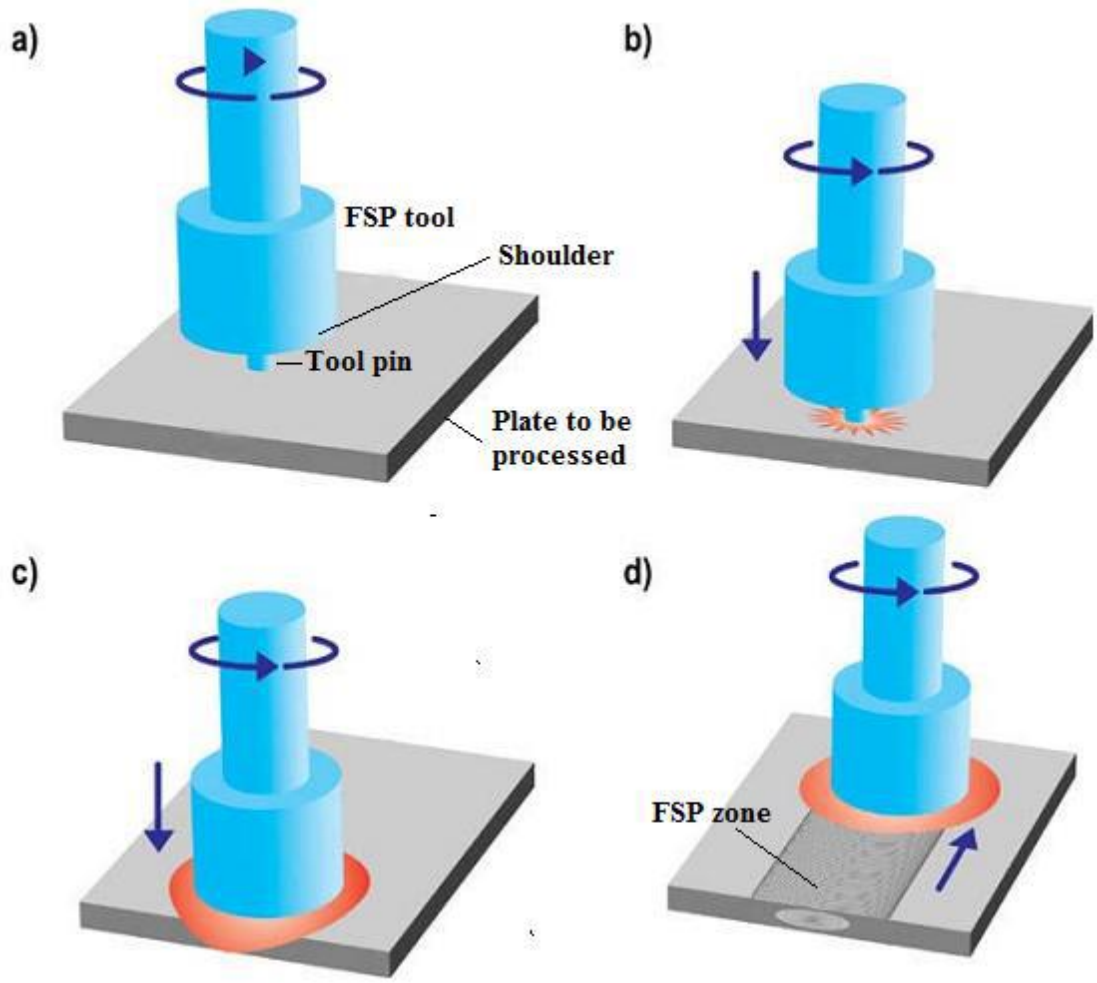

Figure 1.6: Steps of FSP (a) rotating tool prior to contact with the plate (b) tool pin makes contact with the plate, creating heat (c) shoulder makes contact, restricting further penetration while expanding the hot zone and (d)plate moves relative to the rotating tool, creating FSP [33]

1.7 Objectives

Fabrications of copper-graphite MMC by friction stir processing using Cu and graphite as starting materials.

Effect of various parameters like Tool tilt, RPM and feed.

Study the interface between Cu and graphite.

Study of mechanical properties via Tensile and Hardness Testing.

Study of wear resistance of the fabricated composites.

Determining optimal parameters for the better processing via Taguchi method.

Chapter-2

2.1 Literature Review

The section provides an extremely through review of published journals on the effect of process parameters on friction stir processing of copper material. It includes various types of limitations and the approaches adopted for the study of the effect of various parameters.

The process of production of large number of items requires removing the excess material from the raw material. The activity involves large number of machine as well as human parameters which makes it complex phenomenon. The production activity determines the overall cost of the basic product. In the age of competition the cost has to be minimal. To achieve this production activity needs to be optimized in terms of cost/time. The cost/time of production depends upon human parameters such as competency level and wages whereas the more important part is process parameters. These parameters apart from the production rate, influence quality of finished product during a machining operation. To study the influence of various parameters involved one needs to find out from the available data, the practice involved and the shortcomings if any and the possible remedial measures[22].

SNo.	Author	Material Used	Tool Used	Parameters	Observations
3.	Development of high strength, high conductivity copper by friction stir processing K. Surekha , A. Els-Botes	3mm thick pure copper plate was friction stir processed to a depth of 2.8 mm.	High-speed tool steel whose shoulder diameter is 12 mm and pin diameter and length are 5 and 2.8 mm respectively.	Copper plate was friction stir processed to a depth of 2.8 mm by using low-heat input conditions by changing the traverse speed from 50 - 250 mm/min at a constant rotational speed (300 rpm) .	Aims to obtain a high strength, high conductivity copper by friction stir processing. Grain size of the nugget decreased from 9 to 3 micro m and the hardness increased from 102 to 114 HV by increasing the traverse speed from 50 to 250 mm/min. Yield strength, microhardness and ultimate tensile strength increased with decrease in grain size. Electrical resistivity measurement at room temperature showed that there was no change in the resistivity of the processed samples compared to the base metal.
4.	Developments of nanocrystalline structure in Cu	Copper plate thickness of 6mm.	H13 steel and hardened to HRC 52 which was fabricated by the	Copperplate(6mm) was reduced to 2mm in three rolling passes with 30 min anneals at 500 ◦C	Using small tools and imposing rapid cooling, nanocrystalline structures were successfully produced in pure copper in a single

	during friction stir processing (FSP) Jian-Qing Sua, T.W. Nelson, T.R. McNelley, R.S. Mishra[		Tool with shoulder diameter-7.5mm, pin diameter-2.5mm and pin length of 2.0mm.	after each rolling pass, providing a final annealed microstructure with a grain size of 70 nm. The tool was tilted to 2.5° whose direction is opposite to the traveling direction during a single processing pass on the Cu sheet at 800rpm and a travel speed of 120mmmin^{-1}.	step. The resulting microstructures consist of equiaxed, nearly random oriented grains surrounded by high-angle boundaries. The grain size ranges mainly from 50 to 300nm with an average size of about 109nm and 174nm respectively.
5.	H. Khodaverdizadeh , A. Mahmoudi , A. Heidarzadeh , E. Nazari, [2012] Effect of friction stir welding (FSW) parameters on strain hardening behavior of pure copper joints.	Pure copper plate with a thickness of 5 mm.	High speed steel tool .	Two traverse speeds of 25 and 75 mm/min at constant rotation rate of 600 rpm and two rotation rates of 600 and 900 rpm.	Aims to predict the effect of tool rotation rate and traverse speed on strain hardening behavior of friction stir welded copper joints were investigated using hardening capacity and strain hardening exponent concepts. Kocks–Mecking type plots were used to show different stages of strain hardening. FSW samples reveals higher hardening capacity and lower strain hardening exponent relative to base metal. With increasing rotation rate and/or decreasing traverse speed, FSW samples show higher hardening capacity and lower strain hardening exponent. The strain hardening behavior was discussed by dislocation density and grain size variation during FSW.
6.	Heidarzadeh, T. Saeid, [2013] Prediction of mechanical properties in	Pure copper plates of 2 mm thickness with UTS of 272 MPa, TE of 42% and	square tool pin profile	The three welding parameters considered were rotational speed, welding speed, and axial force.	Aims to predict the mechanical properties of friction stir welded pure copper joints. Microstructural characterization and

	friction stir welds of pure copper,Materials and Design	hardness of 102 HV used			fractography of joints were examined using optical and scanning electron microscopes. Also, the effects of the welding parameters on mechanical properties of friction stir welded joints were analyzed in detail. The increase in welding parameters resulted in increasing of tensile strength of the joints up to a maximum value. Elongation percent of the joints increased with increase of rotational speed and axial force, but decreased by increasing of welding speed, continuously. In addition, hardness of the joints decreased with increase of rotational speed and axial force, but increased by increasing of welding speed.
7.	Characterization of oxide dispersion strengthened copper based materials developed by friction stir processing M.-N. Avettand-Fènoël ,A. Simar , R. Shabadi , R. Taillard , B. de Meester	Yittrium particles, Copper flat	a tool made of tool steel tilted backwards by 1^0. The tool was composed of a 20 mm diameter scrolled shoulder prolonged by a 3 mm long cylindrical M6 threaded.	40 mm/min advancing speed, a low rotational rate of 500 rpm and a constant vertical tool penetration.	Aims to show for the first time the ability of friction stir processing (FSP) in incorporating yittrium particles into copper to produce an oxide dispersion strengthened material. The microstructure of the developed composites was characterized at various scales by light microscopy, electron probe microanalysis (EPMA) and scanning and transmission electron microscopy. The increase of the number of FSP passes leads to a more homogeneous and finer distribution of the particles as it favored the dissociation of the clusters

					of initial powder particles and the intergranular fracture of individual elemental particles.
8.	Hamed Pashazadeh , Jamal Teimournezhad , Abolfazl Masoumi, [2013] Numerical investigation on the mechanical, thermal, metallurgical and material flow characteristics in friction stir welding of copper sheets with experimental verification.	Pure copper to alloy will produced, along with the process control required for a successful FSP.	Tool material H13. The tool pin and shoulder were made of tungsten carbide (WC) and HSS respectively.	The following assumptions were used:(1) a Rigid–Visco- Plastic (RVP) material model is selected as the workpiece; (2)the FSW tool and the backing plate are rigid;(3)the friction coefficient is constant; and (4)the thermal properties s of the workpiece and FSW tool are constant.	Aims to predict the hardness of a copper workpiece undergoing butt joint Friction Stir Welding (FSW). Hardness measurements and microstructural evaluations were performed on the welded specimens. Also a 3D Arbitrary Lagrangian Eulerian (ALE) numerical model was developed to obtain hardness values. Numerical results for hardness values showed good agreement with recorded experimental data. The main part of material flow occurs near the top surface. Material near the top surface at the behind of tool stretches from retreating side towards advancing side, leads to non-symmetrical shape of the stir zone.
9.	Prediction of mechanical and wear properties of copper surface composites fabricated using friction stir processing R. Sathiskumar , N. Murugan , I. Dinaharan , S.J. Vijay	Pure copper plates of length-100mm, width-50mm and thickness-6mm & five different ceramic particles such as SiC , TiC , B4C, WC and Al2O3 were used .	A tool made of double tempered H13 hot working steel with a cylindrical pin profile.		Aims towards successfully applying FSPed to prepare copper surface composites reinforced with variety of ceramic particles such as SiC, TiC, B4C, WC and Al2O3. Empirical relationships are developed to predict the effect of FSP parameters on the properties of copper surface composites such as the area of the surface composite, microhardness and wear rate. B_4C reinforced composites have higher microhardness and

					lower wear rate. Higher tool rotational speed, lower traverse speed and minimum groove width yielded higher area of surface composite.
10.	I. Galvao, A. Loureiro and D. M. Rodrigues, [2012] Influence of process parameters on the mechanical enhancement of copper-DHP by FSP.	Copper plates,1 mm-thick and 250 mm- long, were butt joined by friction stir welding.	Three tools with a 3mmdiameter and 0.9 mm-length right-handed-thread cylindrical pin and a 13 mm-diameter shoulder were used.	The welds were performed in an ESAB Legio FSW machine with a maximum vertical down force of 25 KN. A tool tilt angle of 2◦ was used for the flat and concave tools and 0◦ for the scrolled tool, in order to drive the material flow better. The tool rotation speed (W) was varied in the range of 400–1000 rev min−1 and the traverse speed (v) between 160 and 250mmmin^{-1}	The aim of this work is to study the influence of the shoulder geometry on friction stir welding of 1mmthick copper-DHP plates. The welds were produced using three different shoulder geometries, flat, conical and scrolled, and varying the rotation and traverse speeds of the tool.
11.	Friction stir forming to fabricate copper–tungsten composite by Yogita Ahujaa, Raafat Ibrahima, Anna Paradowskab, Daniel RileybaMonash	Oxygen free copper (C1100) blocks with a dimension of 80 mm×50 mm×12 mm were used for conducting the FSF	100 mm long probeless tool with an 8◦ concave shoulder wa manufactured from H13 tool steel.	Mid-range value of 0.05 mm plunge depth, 3◦ tilt angle, 970 rpm tool rotation speed and 100 mm min−1 tool traverse speed, was set as the reference parameter combination.	Tungsten embedded composite of copper was fabricated through probe less tool aided friction stir forming (FSF). Preliminary FSF of copper was performed by varying the tool plunge depth and tilt angle. Tool rotation and traverse speed were kept constant at 970 rpm and 100 mm min−1 respectively. No plastic deformation occurred at the low plunge depths of 0.025 mm and 0.05 mm with 1◦ tool tilt angle. Substantial encapsulation of the cavity can be observed at the higher tool rotation speed. Grain

					refinement induced work hardening was observed in the copper close to the interface. The bond strength of the Cu–W mechanical interlock fabricated by FSF was determined to be 130 MPa.
12.	Flow visualization and estimation of strain and strain-rate during friction stir process S. Mukherjee, A.K. Ghosh	Two 101.6mm×101.6mm×8mm 5083 aluminum plates and a 101.6mm×8mm×0.29mm aluminum foil which is sandwiched between them.	The FSP tool has a cylindrical flat shoulder and a conical pin with a spiral groove.	A tool rotation of 1500RPM and a feed rate of 50.8mm/min are employed in all experiments. The tool is tilted 2◦ towards the backside with respect to the plate surface normal during FSP.	Soft and ductile aluminum foil is embedded within a workpiece undergoing friction stir processing (FSP) to observe the deformation zone. A whirlpool of material is detected in the stir zone which consumes the foil over time. Additionally a strain-rate is numerically evaluated from the FSP process parameters and the deformed foil geometry using finite-element analysis.
13.	Masoud Jabbari, [2014] Elucidating of rotation speed in friction stir welding of pure copper	Pure copper plates. With Chemical composition of Cu 99.85 Ni 0.08 Zn 0.041 Si 0.007 Al 0.006 Fe 0.006 Mn 0.006 B 0.002 Sb 0.001 .	Pin diameter 5 mm Shoulder diameter 15 mm Pin length 3.95 mm Pin shape Cylindrical pin.	welding was carried out in constant traverse speed of 25 mm/min with different rotation speed of 400, 600, 900, 1200 and 1500 rpm.	In this paper, a thermal model is developed and used to simulate the friction stir welding of pure copper plates with the thickness of 4 mmin the constant traverse speed of 25 mm/min and five different rotation speeds. The mechanical deformation (plastic deformation) is neglected in the developed thermal model; hence the mechanical force in the process is taken to account in the heat generation equations.
14.	Mohsen Barmouz, Mohammad Kazem Besharati Givi, [2011]	In this study, the material used was a pure copper plate with 130mm length, 75mm	A FSP tool was made of hot working steel with the shoulder diameter, square pin	A processing tool was tilted by an angle of 2°.The FSP parameters were varied from 710 to 1120 rpm in tool rotational speed	Aim of this study is to produce copper reinforced metal matrix composite (MMC) layers using micron sized SiC particles via friction stir processing (FSP) in order to enhance surface

	Fabrication of in situ Cu/SiC composites using multi-pass friction stir processing: Evaluation of microstructural , porosity, mechanical and electrical behavior.	width and 6mm thickness.	diameter and length of 20, 5 and 2 mm, respectively.	and 40 to 200 mm/min in traverse speed.	mechanical properties. Microstructural evaluation using optical microscopy (OM) and scanning electron microscopy (SEM) indicated that an increase in traverse speed and a decrease in rotational speed cause a reduction in the grain size of stir zone (SZ) for the specimens friction stir processed (FSPed) without SiC particles. Results were higher microhardness values and enhanced tensile properties were caused by higher number of FSP passes. It was also found that the average friction coefficients of composites fabricated by multi-pass FSP were noticeably reduced compared to the pure copper.
15.	Enhanced strength and ductility of friction stir processed Cu–Al alloys with abundant twin boundaries P. Xue, B.L. Xiao and Z.Y. Ma	Two Cu–Al alloys.	High speed steel tool material	Rotational speed - 600 rpm and a traverse speed-50 mm per min using a tool with a shoulder of diameter-12mm.	Aims to prepare ultrafine-grained Cu–Al alloys via friction stir processing (FSP) with additional rapid cooling. Overlapping FSP did not exert a significant effect on the microstructure and mechanical properties of the FSP UFG Cu. These FSP Cu–Al alloys exhibited equiaxed recrystallized grains with relatively low dislocation density and a high fraction (96%) of high-angle grain boundaries. A high yield strength of 310 MPa and a uniform elongation of 13% were achieved in the bulk FSP UFG Cu
16.	P. Xue, B.L.	Pure Cu (w99.9%)	The rotation tool was made	Two different FSP schemes were	Large-area bulk ultrafine grained (UFG) pure Cu was

	Xiao, Z.Y. Ma, [2013] Achieving Large-area Bulk Ultrafine Grained Cu via Submerged Multiple-pass Friction Stir Processing, J. Mater. Sci. Technol.	plate, 5 mm in thickness, 300 mm in length and 100 mm in width	of heat-treated tool steel (M42) a tool with a shoulder of 20 mm in diameter and a cylindrical threaded pin of 6 mm in diameter and 2.7 mm in length.	followed: single-pass, and 5-pass with half of the pin diameter overlapping. FSP was performed at a rotation rate of 400 r/min and a traverse speed of 50 mm/min.	successfully prepared by multiple-pass overlapping friction stir processing (FSP) under additional rapid cooling. Overlapping FSP did not exert a significant effect on the microstructure and mechanical properties of the FSP UFG Cu.
17.	Article Effect of ceramic particulate type on microstructure and properties of copper matrix composites synthesized by friction stir processing Issac Dinaharan, Ramasamy Sathiskumar, Nadarajan Murugan	pure copper plates of 100 mm length,50 mm width and 6 mm thickness.	A tool made of double tempered hot working steel was used .The tool had a shoulder diameter of 20 mm, pin diameter of 5 mm and pin length of3 mm	The process parameters employed were tool rotational speed of 1000 rpm, travel speed of 40 mm/min and axial force of 10 kN.	The present work aim to produce copper matrix composites (CMCs) using FSP and analyze the effect of ceramic reinforcement type (SiC, Al2O3, B4C and TiC) on the evolving microstructure, microhardness and wear resistance behavior. A groove was made on 6 mm thick copper plates and packed with various ceramic particles. A single pass FSP was carried out using a tool rotational speed of 1000 rpm, travel speed of 40 mm/min and an axial force of 10 kN. The microstructure and distribution of the ceramic particles were studied using optical and field emission scanning electron microscopy. The sliding wear behavior was evaluated using a pin-on-disk apparatus. The results indicate that the variation in the stir zone, distribution, grain size, hardness and wear resistance of CMCs were within a short range. Nevertheless, Cu/B4C CMC

					exhibited superior hardness and wear resistance compared to other CMCs produced in this work under the same set of experimental conditions.
18.	Influence of rotational speed on the formation of friction stir processed zone in pure copper at low-heat input conditions S. Cartigueyen, K. Mahadevan	commercial pure copper plates of 150 mm length, 50 mm width and 6 mm thickness were used for FSP	The FSP tool was fabricated from high carbon high chromium (HCHCr) tool steel followed by hardening and tempering process to increase the hardness to 55–58 HRC.	plunge of 0.1 mm depth rotational speeds 250-500 rpm.	The influence of rotational speed on the formation of friction stir processing (FSP) zone in commercial pure copper at low-heat input conditions. The experiments were conducted using K-type thermocouples to record the peak temperature history at different locations on the workpiece. The results suggest that the temperature achieved during processing plays an important role in determining the microstructure and properties of the processed metal. FSP produced very fine and homogenous grain structure and it is observed that smaller grain size structure is obtained at lower rotational speed whereas a tunnel defect was formed at lower speed of 250 rpm. It is also observed that the hardness of the processed copper depends strongly on the heat input during FSP.
19.	R. Sathiskumar, N. Murugan, I. Dinaharan, S.J. Vijay, [2013] Characterizatio n of boron carbide particulate	FSP technique has been successfully applied to prepare copper surface composites reinforced with variety of	A pin less tool was initially employed to cover the top of the groove after filling the ceramic particles to prevent them from scattering	A central composite rotatable design consisting of four factors and five levels is used to minimize the number of experiments. The factors considered are tool rotational	Empirical relationships are developed to predict the effect of FSP parameters on the properties of copper surface composites such as the area of the surface composite, microhardness and wear rate

	reinforced in situ copper surface composites synthesized using friction stir processing.	ceramic particles such as SiC, TiC, B4C, WC and Al2O3.	during FSP. A tool made of double tempered H13 hot working steel with a cylindrical pin profile. The tool had a shoulder diameter of 20 mm, pin diameter of 5 mm and pin length of 2.7 mm.	speed, traverse speed, groove width and type of ceramic particle. Rotational speed (rpm)800, 900, 1000, 1100, 1200, Traverse speed (mm/min) 20, 30, 40, 50, 60.	
20.	S. Mukherjee, A.K. Ghosh, [2011] Friction stir processing of direct metal deposited copper–nickel 70/30.	DMD-Deposited copper–nickel 70/30 on a copper–nickel 70/30 substrate.	Tungsten alloy tool with scrolled shoulder and scrolled pin. The shoulder diameter was 15mm.The conical pin had a base diameter of 3.5mm and a tip diameter of 1mm. The pin height was 3.1mm from the surface of the shoulder. The tungsten alloy has a high melting point (3120 ◦C) and a low ductile-to-brittle transition temperature which makes it an ideal candidate for FSP tool material. The tool was cooled using a continuous supply of water	FSP was carried out at a tool rotation rate of 1200rpm counterclockwise. Three different feed rates, namely, 12.7 mm/min, 25.4mm/min and 50.8mm/min were used. The tool was tilted 3◦ towards the backside with respect to the surface normal during FSP.	Aims to predict the microstructural changes associated with single and overlapping FSP passes which were analyzed using electron microscopy. Mechanical property and corrosion behavior were also evaluated before and after FSP. It was observed that FSP reduces porosity, refines grains, increases hardness, reduces ductility and increases corrosion rate in comparison to DMD copper–nickel 70/30.

			to prevent		
21.	Effect of friction stir processing parameters on the microstructural and electrical properties of copper R. M. Leal1,2 & I. Galvão1 & A. Loureiro1 & D. M. Rodrigues.	Copper C12200, temper class H02	conical and scrolled shoulder tools	tool rotation speeds of 400, 750 and 1000 rpm and tool traverse speeds of 160 and 250 mm/min, plunge force of 7000 N was used for both tools	Friction stir processing (FSP) which can be used for changing locally the microstructure and the mechanical properties of conventional materials. In this work, the copper alloy C12200 was friction stir processed using two distinct tools, i.e. a scrolled and a conical shoulder tool, in order to promote different thermomechanical conditions inside the stirred volume, and consequently, varied post-processed microstructures. The influence of the tool geometry and tool rotation and traverse speeds on the microstructural and electrical properties of the processed copper alloy was analysed. The processing conditions were found to have an important influence on the electrical conductivity of the processed material.
22.	J.J. Shen, H.J. Liu , F. Cui, [2010] Effect of welding speed on microstructure and mechanical properties of friction stir welded copper, Materials and Design	The base metal (BM) used in the experiment was a pure copper plate (under the 1/2H condition) of 3mm thickness.	The rotation tool was made of high-speed tool steel, with a pin (ϕ/3 x 2.85 mm) having standard right-hand threads and a shoulder (/12 mm) having a concave profile	FSW was conducted at a constant rotation rate of 600 rpm together with different welding speeds of 25, 50, 100, 150 and 200 mm/min.	Influence of welding speed on microstructure and mechanical properties of the joints was investigated. As the welding speed increased, the grain size of nugget zone first increased and then decreased, the thermomechanically affected zone became narrow and the boundary between these two zones got distinct, but the heat affected zone was almost not changed. The ultimate tensile strength and elongation of the joints increased first and

					decreased finally with increasing welding speed, but the effect was little when the welding speed is in the range of 25–150 mm/min.
23.	Effect of Single and Multiple-Pass Friction Stir Processing on Microstructure, Hardness and Tensile Properties of a 99.99% Cu with Carbon Nano Tubes by V. Jeganathan Arulmoni, R. S. Mishra	Copper plate that is used for processing 200 mm x 74 mm x 5 mm.	The tool Material used is H13 steel with shoulder diameter 15mm, threaded pin diameter 8 mm, pin length 2.5 mm	Tool rotational speed 960 rpm, tool angle 20 and table traverse speed 25 m / min	The states of development of FSP for processing of Copper with carbon nanotubes are addressed. This paper investigates the parameters affecting the friction stir processed copper with carbon nano tubes and enhancement of the microstructure, hardness and tensile properties of the composite material. The behaviour of Copper with carbon nano tubes has been studied with single pass, double passes and triple passes.

2.2 Summary

- Friction stir welding / processing is a new surface modification technique and resulted in significant grain refinement in the processing material.
- Post-processed microstructural characteristics are highly dependent on the geometry of the processing tool.
- The strength of the FSP material improved significantly and at the same time the ductility was also retained, the hardness also improved substantially.
- FSP was found to be beneficial in improving wear resistance. The high wear behavior in the stir zone is attributed to a lower coefficient of friction and the improved micro-hardness in this region.
- Fracture mechanism of FS processed pure copper significantly depends on grain size and cavity formation during process. Grain size is controlled by heat input and cavity formation decreases with higher plastic deformation, produced by tool.
- Machine parameters considered during FSP are tool travel speed, rotational speed, tilt angle and penetration depth. Out of these, tool travel speed and rotational speed have major effect during FSP. Penetration depth and tilt angle are also considered variable.

CHAPTER-3

3.1 Experimental Set Up:

3.1.1 FSW Machine

An indigenous developed friction stir welding machine (R V machine tools, FSW-4T-HYD, shown in figure 1.5) was used for Friction Stir Processing. Specifications of the machine are as follows:

- Power – 11 KW
- Rpm – 3000
- Load capacity – 25 KN
- Clamps – hydraulic actuated
- Backing plate groove – 200 mm × 80 mm

3.1.2 Tinius Olsen Universal Testing Machine:

- Capacity: 50kN
- Test Speed: Up to 25kN 0.001-500mm/min
  Over 25kN 0.001-250mm/min
- Return Speed: 0.001-500mm/min
- Test Area: Vertical (no tooling) 1100mm
  Horizontal (between columns) 405mm
  Depth Unlimited

3.1.3 Optical Microscope:

The microstructural evolution during the FSP were characterized using an Olympus Optical Microscope (OM), model GX 41 equipped with image analysis software, a camera having 10x, 20x, 50x and 100x lens and a computer.

3.1.4 Pin on Disk Tribometer Specifications

The specification of the machine is as follows:

- Pin diameter of 3, 4, 6, 8, 10 and 12 mm.
- Disc size of 165 mm diameter and 8 mm thickness.
- Disc speed ranging from 200 to 2000 rpm, infinitely variable in steps of 1 rpm.
- Normal load ranging from 1 N to 200 N in steps of 5 N.
- Frictional force ranging from 0 to 200 N.
- Wear track ranging from minimum diameter of 50 mm to maximum diameter of 130mm.
- Sliding speed ranging from minimum of 0.5 m/s to maximum of 10 m/s.

Figure 3.1 Pin on the disk tribometer

3.1.5 FSP Tool Specifications

Tool used during FSP (shown in fig.3.2) has following specifications:

- Shoulder diameter of 20 mm.

- Tool material -Tungsten
- Pin profile is of square.
- Pin size of 6 mm side.
- Pin length is 3 mm.
- Compressive strength- 6.25GPa.
- Density is 14.8g/cm^3.
- Hardness is H30V=1600.

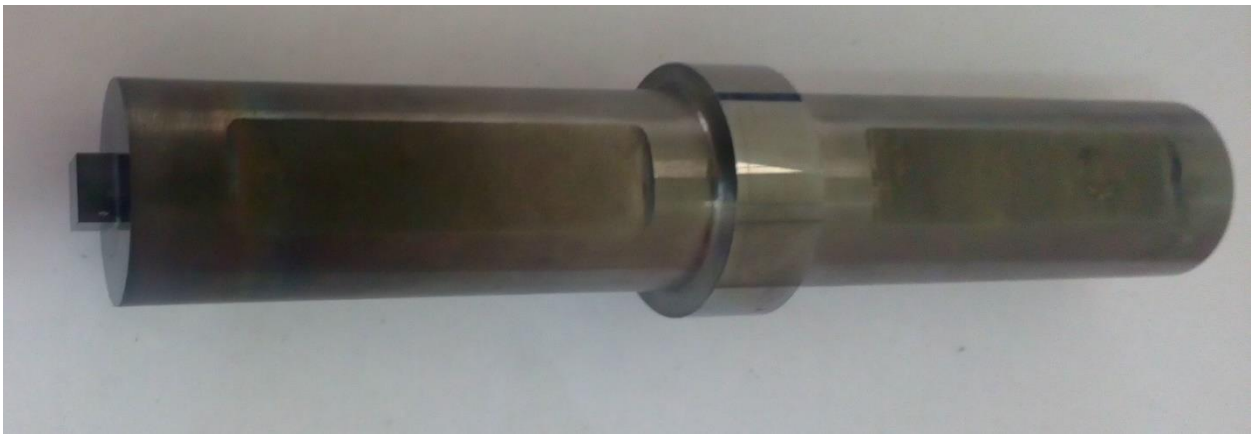

Figure 3.2 Tungsten carbide tool

3.2 Experimental work:

3.2.1 Materials

A pure copper(99%) base plate of 6 mm thickness, 200 mm length and 75mm breadth what's more, fine graphite powder with a normal molecule size of ~ 6 micron meter were utilized as the reinforcement materials.

3.2.2 Procedure

In the first place, two rectangular groove of 1 mm wide and 2.5 mm depth was machined in the copper base plate via milling machine, After this, groove was properly cleaned with acetone which was along these lines firmly pressed with the graphite powder . A pressing (capping pass) was then performed over the graphite-filled groove using a pin-less tool (made of tungsten carbide , 20 mm shoulder diameter).The procedure parameters utilized for the pressing (capping

pass) were: The process parameters used for the capping pass were: 1000 rpm tool rotation speed, 15 mm/min traverse speed, 0° tool tilt . A portion of the imperfections experienced during trial tests.

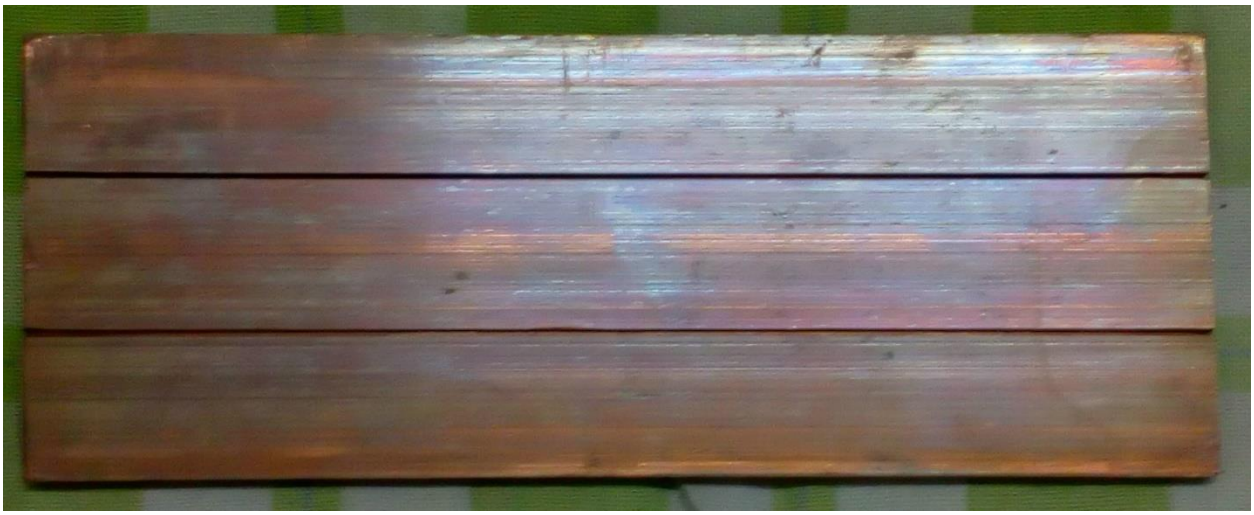

Figure3.3 Grooved copper flat

Figure 3.4 Wire cut copper flat

The pressing (capping pass) was intended to close the section so that the graphite powder does not take off amid FSP. Following this, FSP was done over and along the pressed grove utilizing a tungsten carbide tool consisting of square pin of side 6mm and length of 3mm. five such plates were friction stir processed by varying the process parameters. For every pass, the specimen was allowed to be cooled to the room temperature and all the experiments were carried out at room temperature. The specimen was clamped on the hydraulic fixture with mild steel backing plate.

3.2.3 Volume fraction calculation

Volume fraction of graphite particles used during FSP was calculated from the following expressions given below:

$$\text{Volume Fraction} = \frac{\text{Area of Groove}}{\text{Projected Area of Tool Pin}} \times 100$$

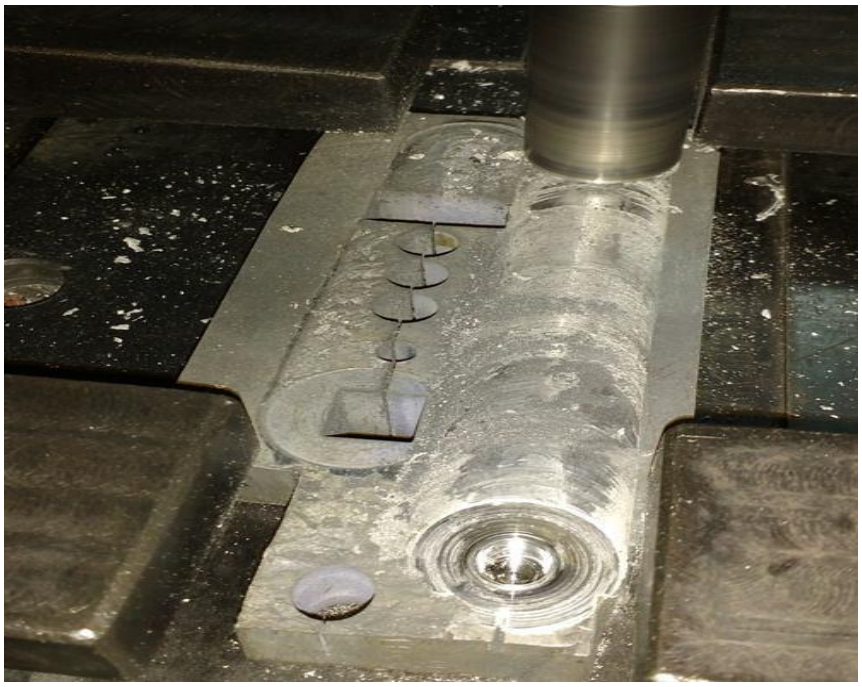

Figure 3.5 Friction Stir Processed Zone.

where, Area of Groove = Groove width × Groove depth

Projected Area of Tool Pin = Pin Size × Pin length

From the above expressions, volume fraction of graphite particles comes out to be nearly 5.56%.

To study microstructure, microhardness and wear; samples were cut in transverse direction

from the middle portion of stirred zone of the FSPed surface with the help of wire EDM as shown in figure 3.8.

3.2.4 Process Parameters

Table for process parameters are given which is derived according to the L9 array of Taguchi method. The parameters are taken along with only single pass considered.

Table 3.1

Process Parameters

	RPM	Traverse Speed	Tool Tilt
Specimen 1	**900**	**20**	**2.0**
Specimen 2	**950**	**25**	**2.0**
Specimen 3	**900**	**25**	**2.5**
Specimen 4	**1000**	**20**	**2.5**
Specimen 5	**950**	**15**	**2.5**
Specimen 6	**900**	**15**	**1.5**
Specimen 7	**1000**	**25**	**1.5**
Specimen 8	**950**	**20**	**1.5**
Specimen 9	**1000**	**15**	**2.0**

3.2.5 Microhardness Test

The dimensions of the specimens for the microhardness test are 10mm diameter cylinder which is carved through the Wire EDM process. Further analysis for Vickers test is done by Spectro Laboratory, Okhla. The microhardness of the bulk FSP pure Cu sample was measured along the middle-thickness of the processed zone with a 10 gram load for 10 seconds.

Figure3.6 Specimens for Microhardness Test

3.2.6 Tensile Test

Tensile specimens were machined from the processed zone in two directions, parallel (longitudinal) to traverse direction. As-processed specimens shows a reduction in yield and ultimate strengths in the stirred zone, while elongation was unaffected. The dimensions of the specimens for the tensile test are which is carved through the Wire EDM process. Large dog-bone-shaped tensile specimens with a gauge length of 33 mm, a gauge width of 6 mm and a gauge thickness of 6 mm were machined perpendicular to the FSP direction from the processed

zone in the bulk sample, and the tensile specimen is schematically shown in Fig. 1. All the tensile tests were conducted.

Figure 3.7 Specimens after tensile test

3.2.7 Microstructure Determination

Specimens of size 10 mm× 10 mm were extracted from the friction stir processed plates via Wire EDM to evaluate microstructure. The specimens were transformed to bigger size via mould making using resins and hardener such that they would be easier to hold while following further polishing and etching processes. For polishing process specimens are rubbed over emery paper nos. 200, 400, 600, 1200. Then onwards it is rubbed with alumina powder with water over polishing machine whose wheel is rotating around 300-400 rpm. Afterwards specimens were polished as per standard metallographic procedure and etched with an etchant containing 5 ml HF, 1 ml HNO_3, 25 ml HCL in 100 ml distilled water and then dried through hot air via blower. Thereafter specimens were safely put in plastic bags for protection from the dust and foreign particles.

Confirming to above procedure specimens were taken to Optical microscope for microstructure determination. The area of the surface composite was measured using an image analyzer using scales of 10x, 20x, 50x and 100x.

3.2.8 Wear Test

Wear samples of 10 mm diameter, which were cut from the stirred zone as discussed above, were small in size and difficult to hold in the wear testing machine. Therefore for easy holding, mild steel pins of 10 mm diameter were used as a dummy as shown in figure 3.11. These dummy pins were mounted on the wear samples as shown in figure 3.11. Mounting was done by drilling a hole of 4 mm diameter and 3 mm deep in the sample with the help of drilling machine; after that sticking of dummy pin to the processed wear samples was done with the help of Araldite and ultimately samples were kept drying for about 24 hours. Finally, filing was done on the flat surface of wear samples to avoid unevenness during wear test. In this way, total 10 wear samples were prepared for wear testing operation. The wear behavior of the surface composites was evaluated by a pin on disc tribometer. Wear test was conducted at load of 50 N, sliding speed of 2.5m/s and sliding distance of 3km.

Figure3.8 Mild Steel Dummy pins

Figure3.9 Pins for wear test

CHAPTER-4

Results and Discussion:

4.1 Particle distribution

Amid fabrication of MMCs by means of FSP, the key issue is setting up a uniform development of high amount of reinforcement particles with a given values of process parameters . Tool specification and process parameters control the metal material flow and combination of material in the processed zone. One of the primary difficulties is to accomplish a uniform dispersion with a solitary pass, however because of the material flow and intermixing modes which are forced by the FSP tool, in this research work it was not able to accomplish a uniform circulation with a solitary pass.

The crown appearance implies that the trueness of the processed zone underneath it. Any deformation on the crown more often than not runs with a looking at imperfection in the processed zone [27]. The crown appearances of processed zone arranged copper with graphite particles are presented. The surface of the crown is not smooth with a few deformities or discontinuities. Half circle striations comparable to those produced in the customary processing process are additionally obvious on the crown. The deformities in the crown amid trail runs can be reasoned through poor material flow amongst progressing and withdrawing side and lacking plasticization of copper. Figure (include fsped pix) depicts the macrostructure of CMCs reinforced with different graphite particles. The processed zone territory which contains the CMC is unmistakably perceptible in each one of the figures. The indications of a depression made before FSP are not seen. It demonstrates the whole arrangement of the composite and constant flow of plasticized material in the midst of FSP. The frictional heat made by the rubbing of shoulder of square pin tool and the shearing of the pin plasticizes the copper material around and underneath the tungsten tool. The rotational and translational development of the tool transports the plasticized copper from moving side to withdrawing side. This material flow at first makes the depression collapse and stir the compacted graphite particles with the plasticized copper. The rate at which the FSP tool turns and feeded results in the powerful mixing inciting the improvement of the composite. It can lead to a conclusion that the sort of graphite particles has no impact on the arrangement of composite amid the FSP procedure.

4.2 Micro-Hardness Test:

Table 4.1

Hardness values for specimens

Specimen Nos.	H_v (Hardness Nos.)
Specimen 1	176
Specimen 2	162
Specimen 3	152
Specimen 4	148
Specimen 5	168
Specimen 6	172
Specimen 7	164
Specimen 8	168
Specimen 9	142
Specimen 10	180

Microhardness test result(shown in the table) gives us trend which depicts that microhardness of the surface composites decreases as the rotational speed is increased from 900rpm to 1000rpm. The microhardness of surface composites reduces because of the presence of the softer graphite particles

4.3 Tensile test: 4.3 Figures for tensile test

Specimen1: Strength- 93.6MPa

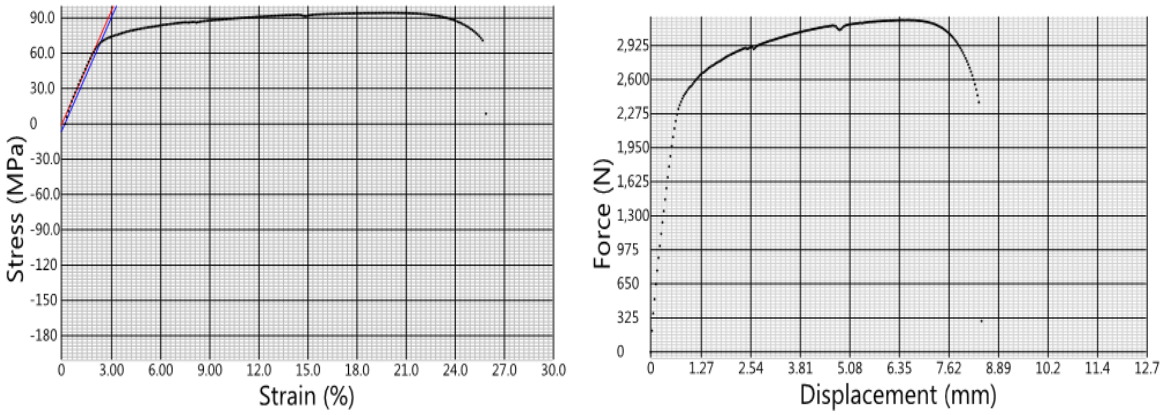

Figure 4.3.1

Specimen2: Strength-149MPa

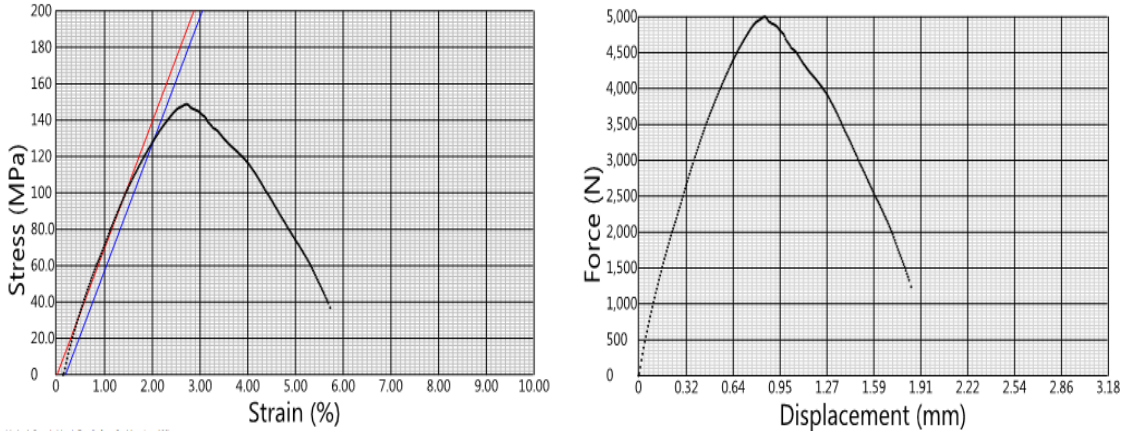

Figure 4.3.2

Specimen 3: Strength-114MPa

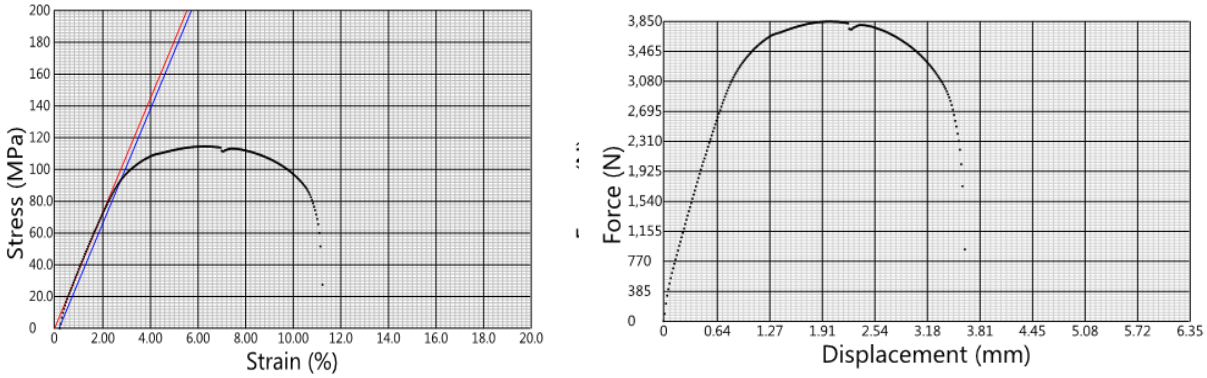

Figure 4.3.3

Specimen 4: Strength-118MPa

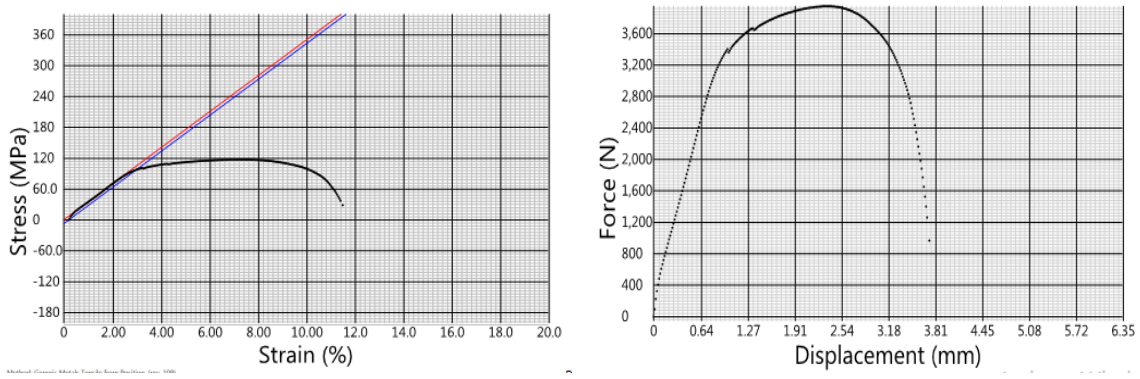

Figure 4.3.4

Specimen 5: Strength-94.3MPa

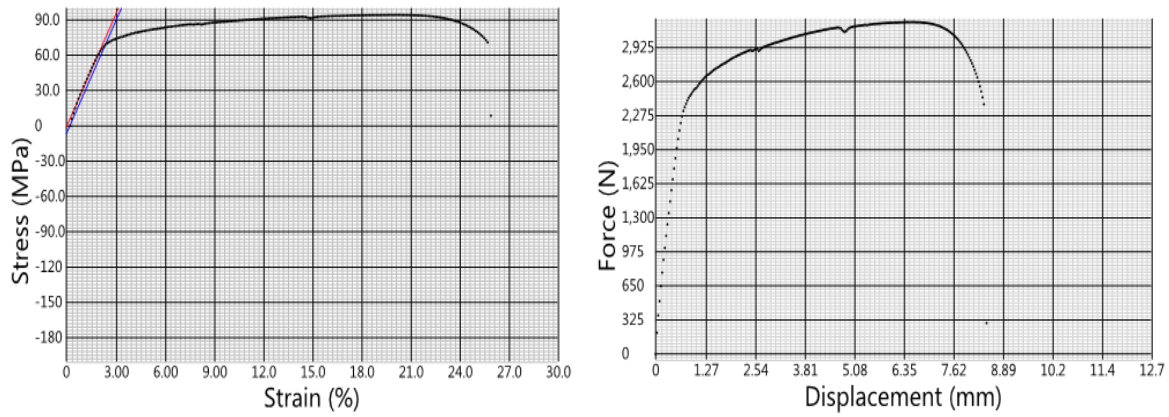

Figure 4.3.5

Specimen 6: Strength-144MPa

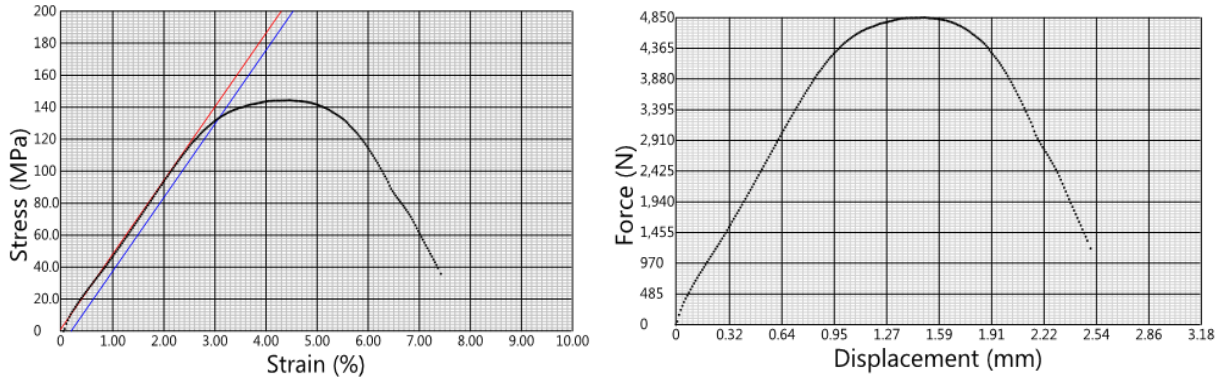

Figure 4.3.6

Specimen 7: Strength-111MPa

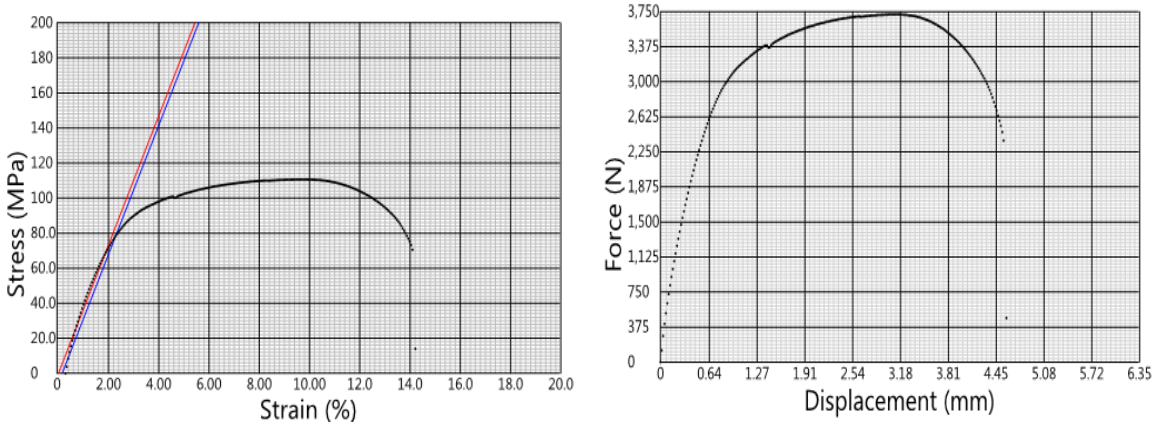

Specimen 8: Strength-108MPa

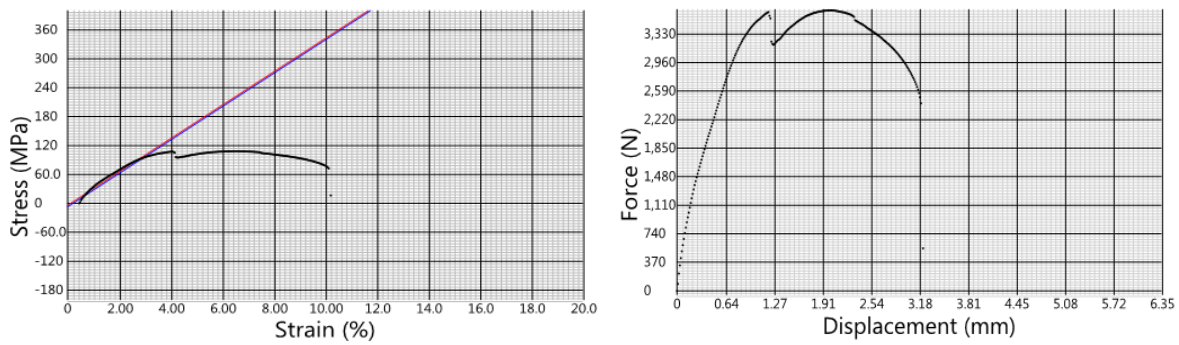

Figure 4.3.8

Specimen 9: Strength-118MPa

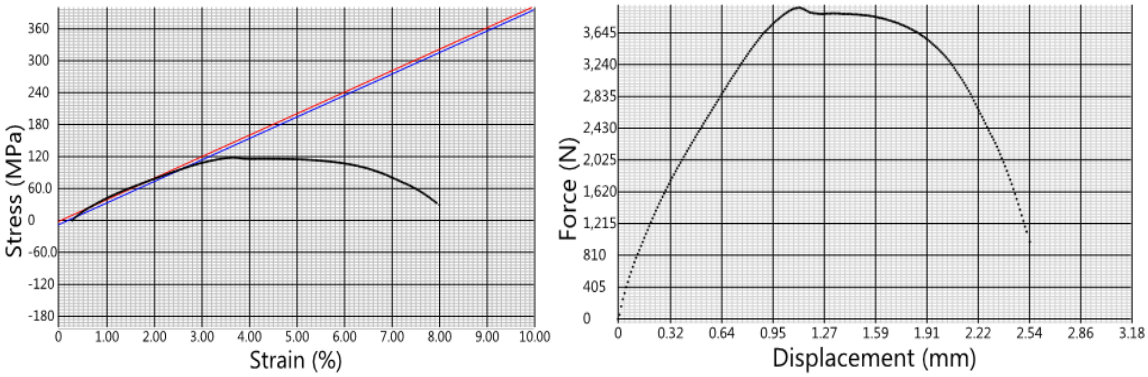

Figure 4.3.9

Specimen 10: Strength-300MPa

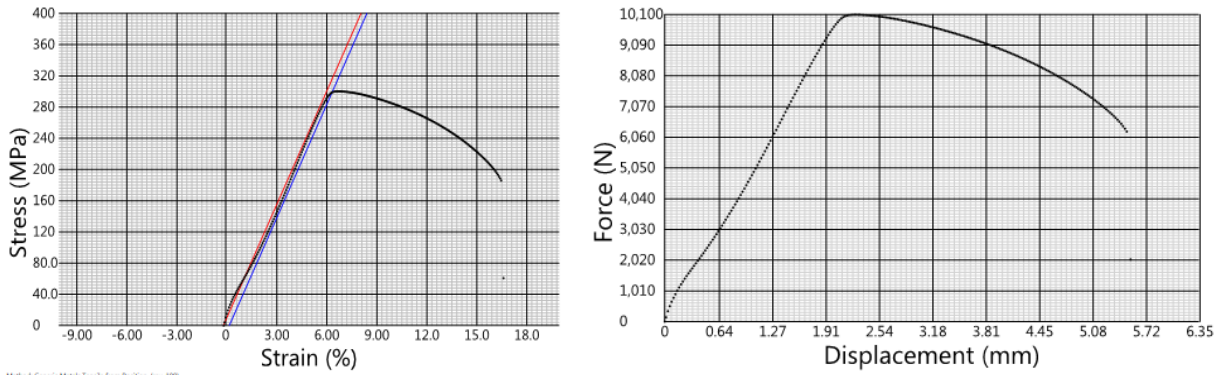

Figure 4.3.10

Table 4.2.1

Values for tensile test

VARIABLES	SPECIMEN 1	SPECIMEN 2	SPECIMEN 3
Thickness in mm	5.60	5.60	5.60
Width in mm	6.00	6.00	6.00
Gauge Length (initial) in mm	33.0	33.0	33.0
Gauge Length (final) in mm	35.5	34.9	36.6
Area in mm^2	33.6	33.6	33.6
Ultimate Force in N	2440	5000	3850
Ultimate Stress in MPa	93.6	149	114
Offset @ 0.2% in N	1900	4340	3130
Offset @ 0.2% in MPa	56.6	129	93.2
TE (Auto) in %	6.94	5.71	10.7
Diameter in mm	N/F	N/F	N/F

Table 4.2.2

Values for tensile test

VARIABLES	SPECIMEN 4	SPECIMEN 5	SPECIMEN 6
Thickness in mm	5.60	5.60	5.60
Width in mm	6.00	6.00	6.00
Gauge Length (initial) in mm	33.0	33.0	34.0
Gauge Length (final) in mm	36.7	41.5	36.5
Area in mm^2	33.6	33.6	33.6
Ultimate Force in N	3950	3170	4850
Ultimate Stress in MPa	118	94.3	144
Offset @ 0.2% in N	3290	2320	4480
Offset @ 0.2% in MPa	97.8	69.0	133
TE (Auto) in %	10.9	25.2	6.83
Diameter in mm	N/F	N/F	N/F

Table 4.2.3

Values for tensile test

VARIABLES	SPECIMEN 7	SPECIMEN 8	SPECIMEN 9	SPECIMEN 10
Thickness in mm	5.60	5.60	5.60	5.60
Width in mm	6.00	6.00	6.00	6.00
Gauge Length (initial) in mm	33.0	33.0	33.0	33.0
Gauge Length (final) in mm	37.6	36.2	35.6	38.5
Area in mm^2	33.6	33.6	33.6	33.6
Ultimate Force in N	3720	3640	3970	10100
Ultimate Stress in MPa	111	108	118	300
Offset @ 0.2% in N	2640	3190	3260	10000
Offset @ 0.2% in MPa	78.5	94.9	96.9	299
TE (Auto) in %	13.6	9.98	7.37	16.5
Diameter in mm	N/F	N/F	N/F	N/F

Above are the tensile test results there is a considerable decrease in the strength of the FSPed composite when compared to standard specimen nos. 10. The drastic decrease in strength of the composite from standard one is obtained. Apart from that other specimen shows expected behavior whose tensile strength value varies from 300MPa for the standard specimen to minimum of 93.6MPa.

4.4 Wear test

The friction coefficient values are significantly decreased with presence of graphite content. Due to mutual sliding of wear counterparts, graphite particles are smeared over contact surface and regarding good lubricating property of graphite, friction coefficient is decreased. It is sticking of graphite particles to sliding surfaces; therefore, sliding take place within interior layers of graphite particles. Infact, a tribolayer is formed on sliding interface which covers the surface. This layer is called mechanical mixed layer(MML).MML reduces the direct contact surface between composite and disk and so friction coefficient and wear loss are decreased. The initial spike in wear plots was due to the metal to metal contact.

Table 4.3

Average friction coefficient values for various specimens

Name	Average Friction Coefficient
Specimen 1	0.268
Specimen 2	0.345
Specimen 3	0.408
Specimen 4	0.309
Specimen 5	0.310
Specimen 6	0.330
Specimen 7	0.168
Specimen 8	0.333
Specimen 9	0.248
Specimen 10	0.490

Table 4.4

Wear rate and wear values

Name	Wear rate(grams/m)	Wear (grams)
Specimen 1	07.30	0.0220
Specimen 2	09.36	0.0281
Specimen 3	10.33	0.0310
Specimen 4	10.10	0.0303
Specimen 5	07.26	0.0218
Specimen 6	09.40	0.0282
Specimen 7	05.26	0.0158
Specimen 8	08.53	0.0256
Specimen 9	06.86	0.0206
Specimen 10	14.46	0.0434

Table 4.5

Wear test process parameters

Specimens nos.	Pin Dia	Load	Speed	Sliding velocity	Track dia	Time
1	10	5	367	2.5	130	1200
2	10	5	398	2.5	120	1200
3	10	5	434	2.5	110	1200

4	10	5	478	2.5	100	1200
5	10	5	530	2.5	90	1200
6	10	5	597	2.5	80	1200
7	10	5	682	2.5	70	1200
8	10	5	796	2.5	60	1200
9	10	5	955	2.5	50	1200
10	10	5	955	2.5	50	1200

The variation of friction coefficient with the sliding distance (m) for all the tested wear samples is shown in the figures. Each plots has a big spike at the initial stages of sliding distance which becomes almost constant after the sliding distance of 1500m. This spike is due to the initial metal-metal contact after some time because of the wear of the parent material all the graphite comes over the surface and induce a layer known as tribolayer which leads to steadiness in the plot and therefore reduced coefficient of friction and enhanced wear resistance as compared to standard raw-copper specimen. The last plot for specimen10 showed some eratic behavior after sliding distance of 1500m which may be due to the internal defects presents in parent specimen.

4.4 Figures from wear test:

Specimen 1:

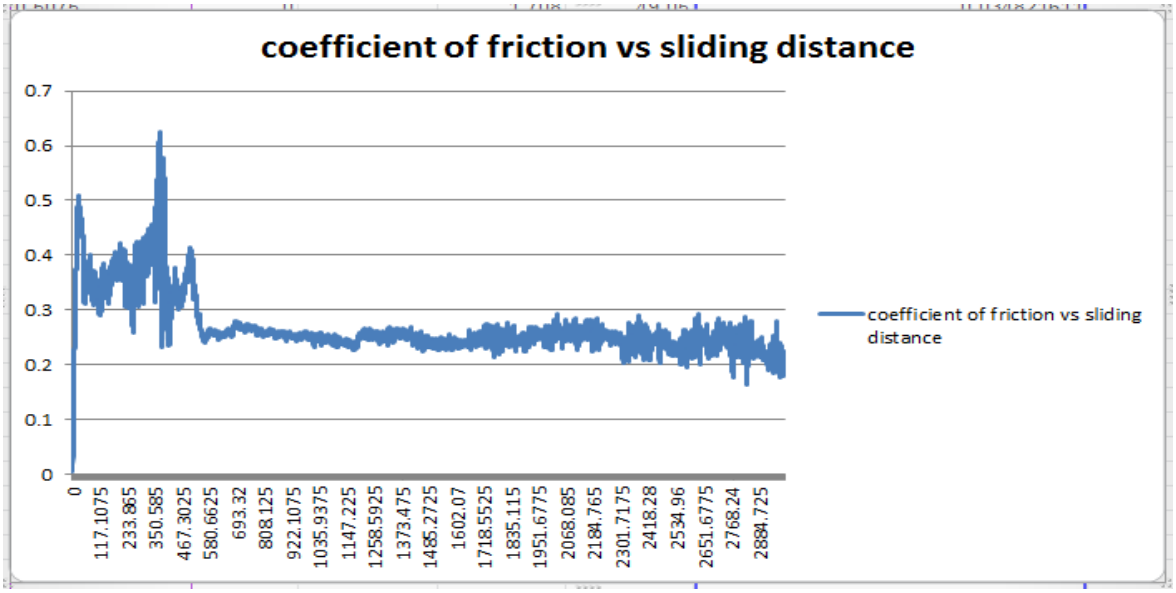

Figure 4.4.1

Specimen 2:

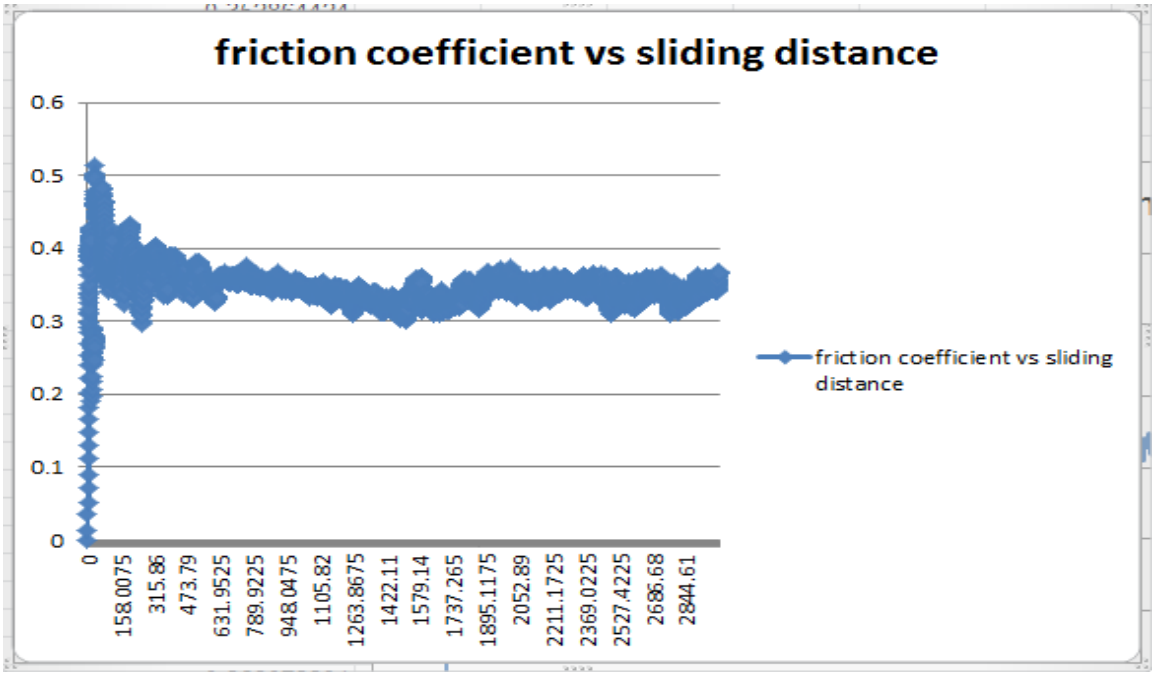

Figure 4.4.2

Specimen 3:

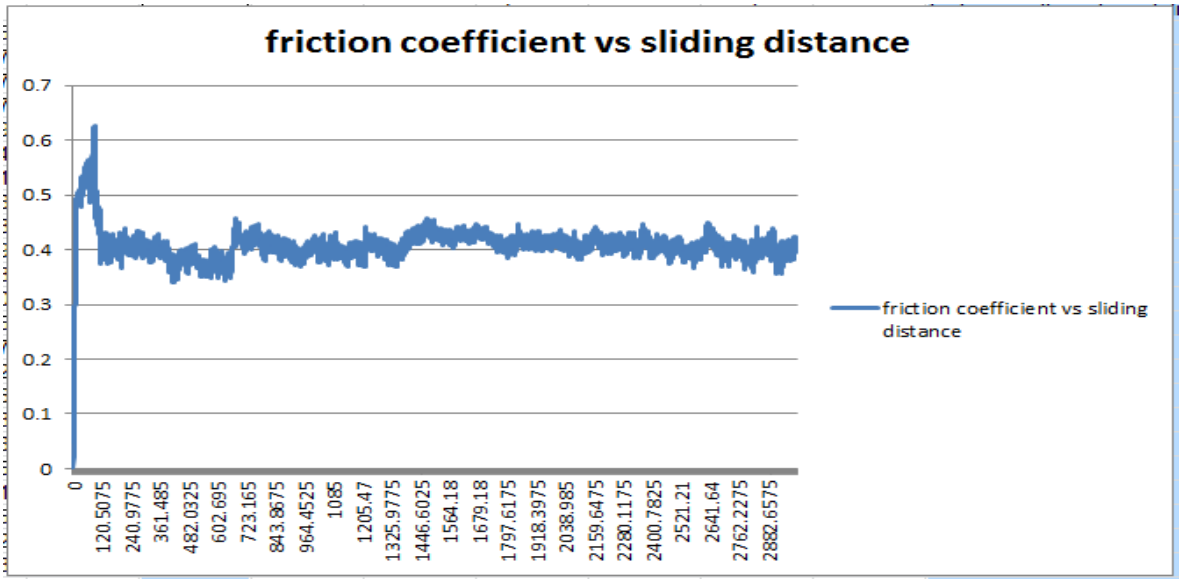

Figure 4.4.3

Specimen4:

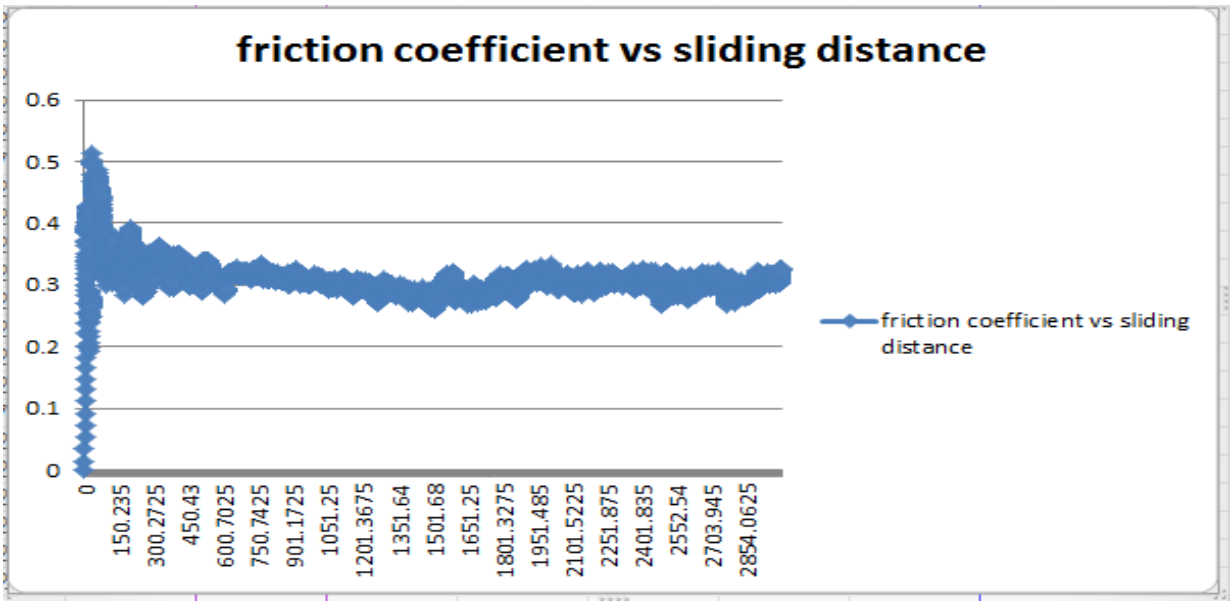

Figure 4.4.4

Specimen 5:

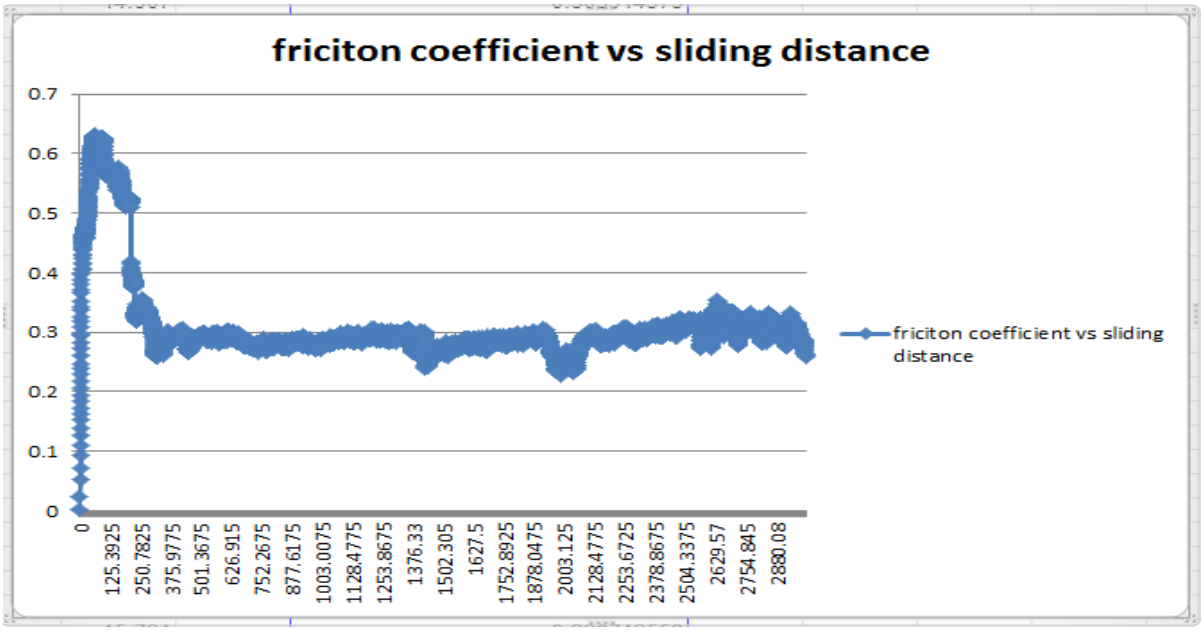

Figure 4.4.5

Specimen 6:

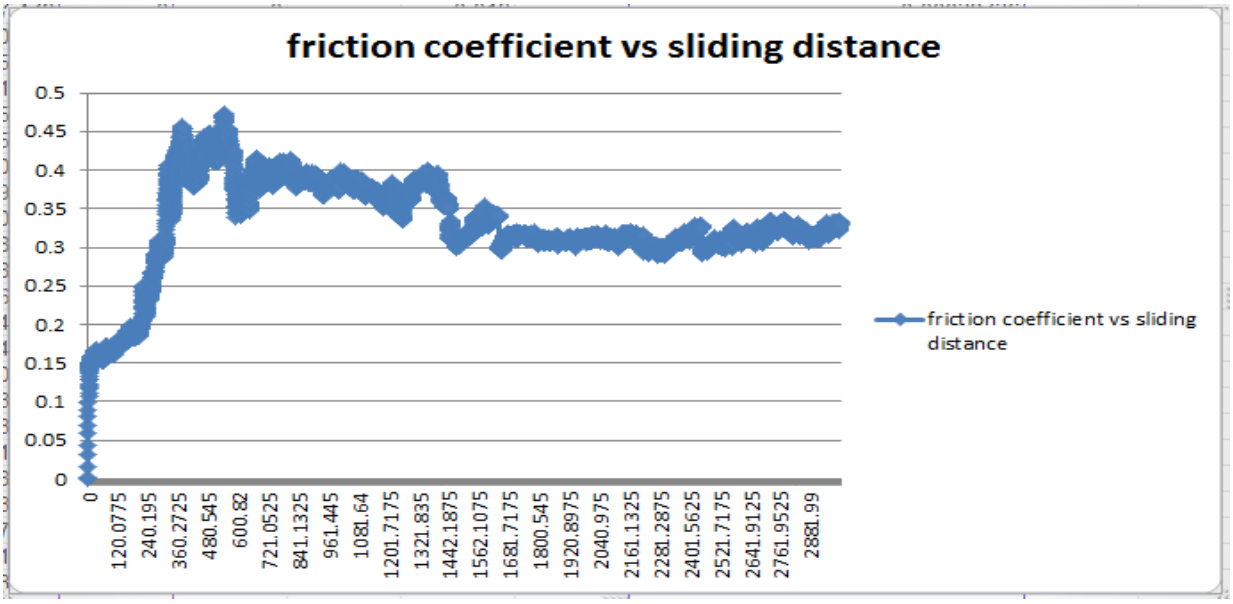

Figure 4.4.6

Specimen7:

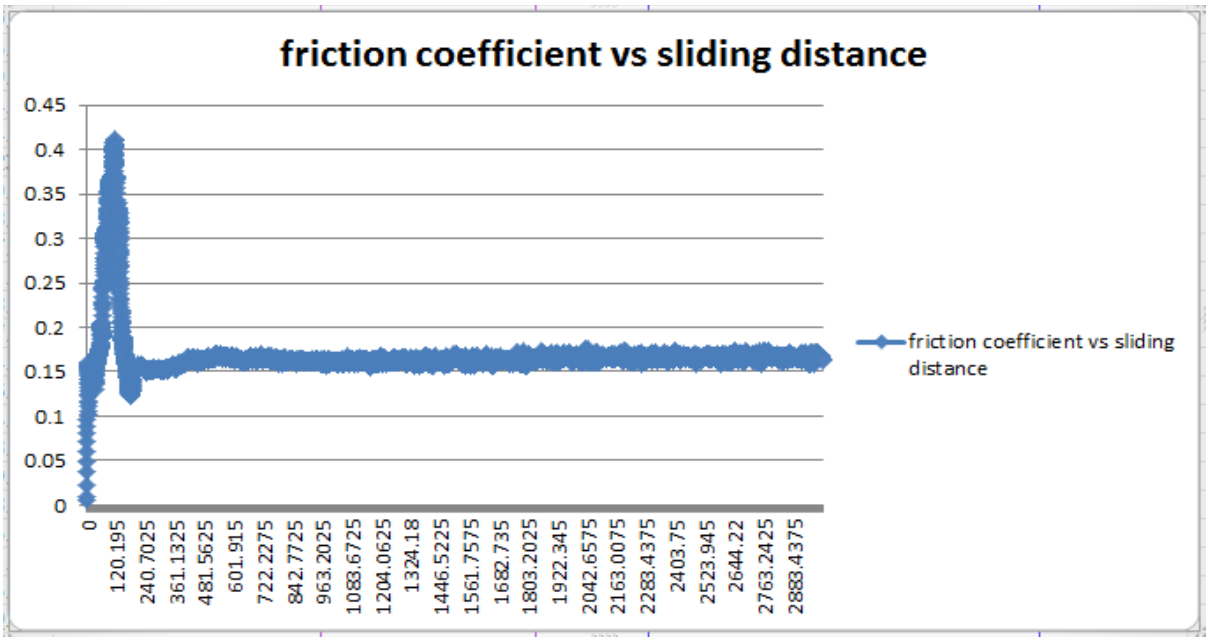

Figure 4.4.7

Specimen 8:

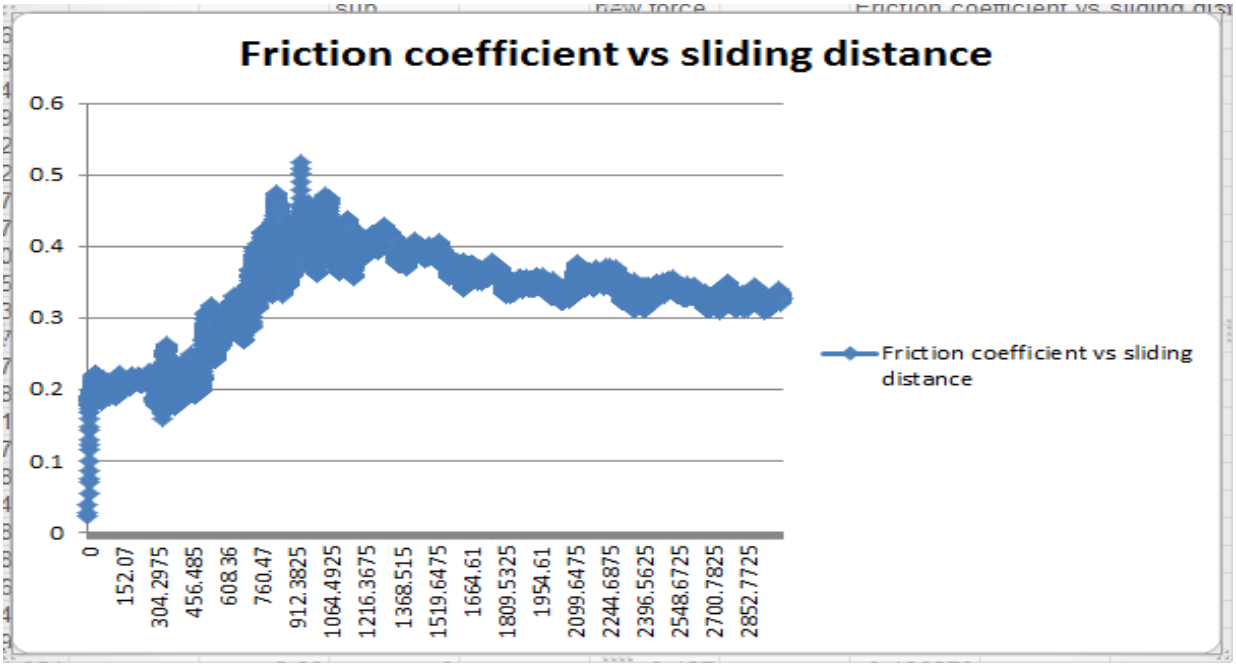

Figure 4.4.8

Specimen 9:

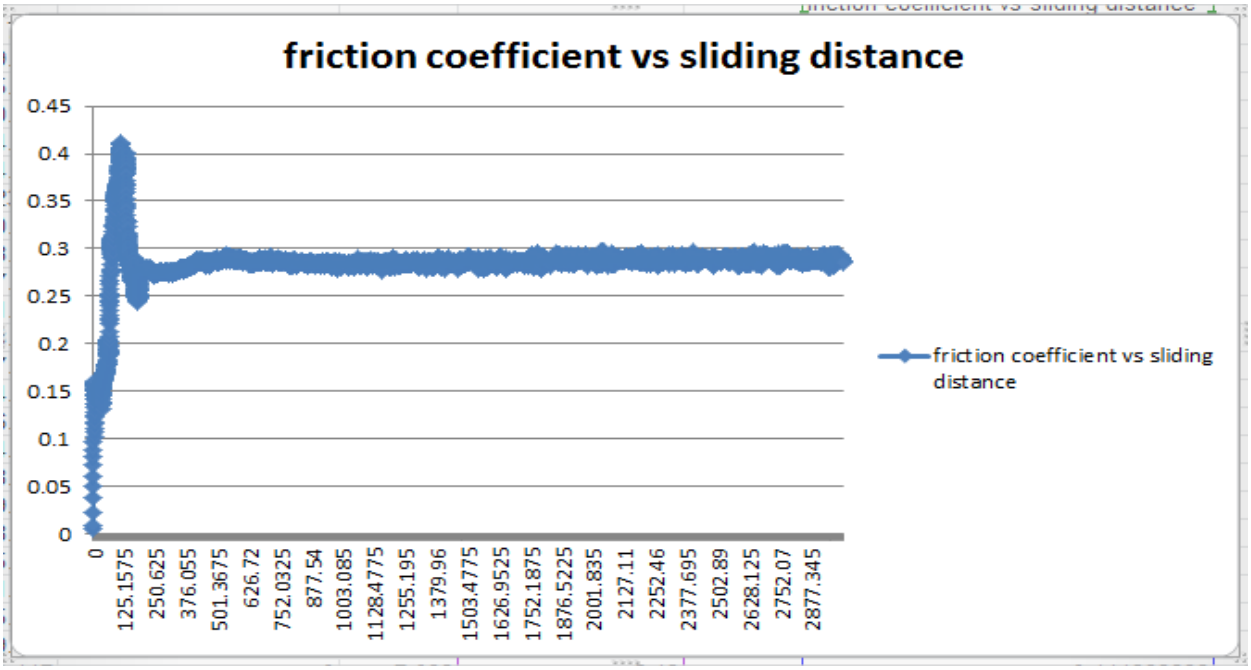

Figure 4.4.9

Specimen 10:

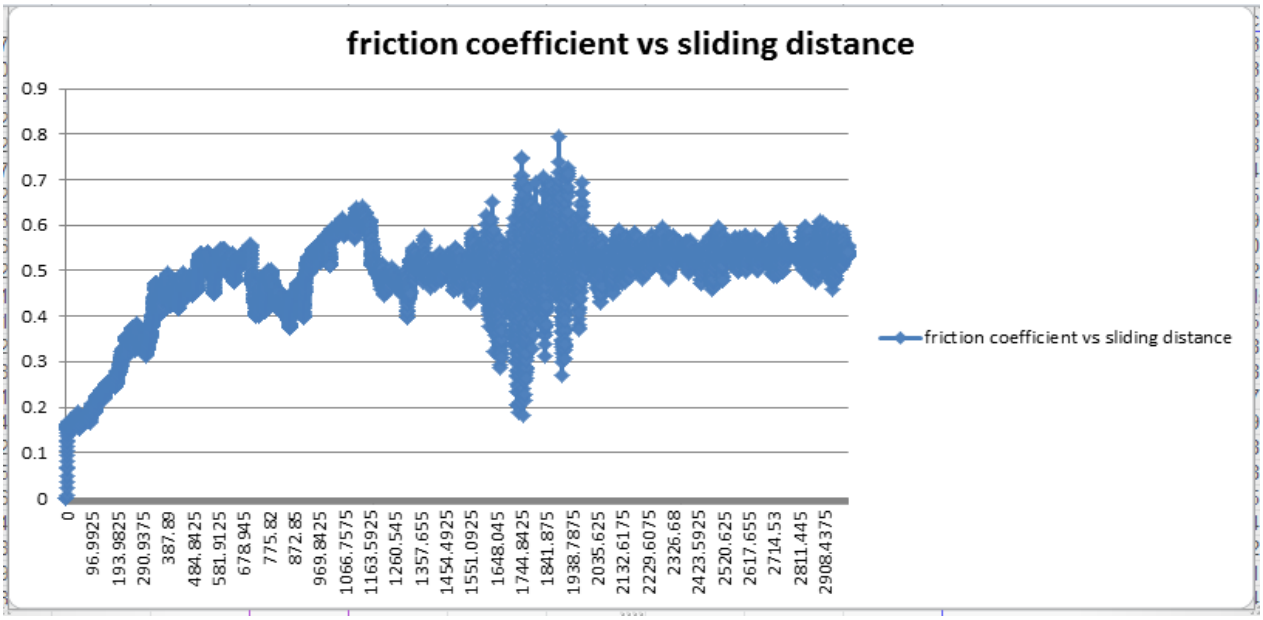

Figure 4.4.10

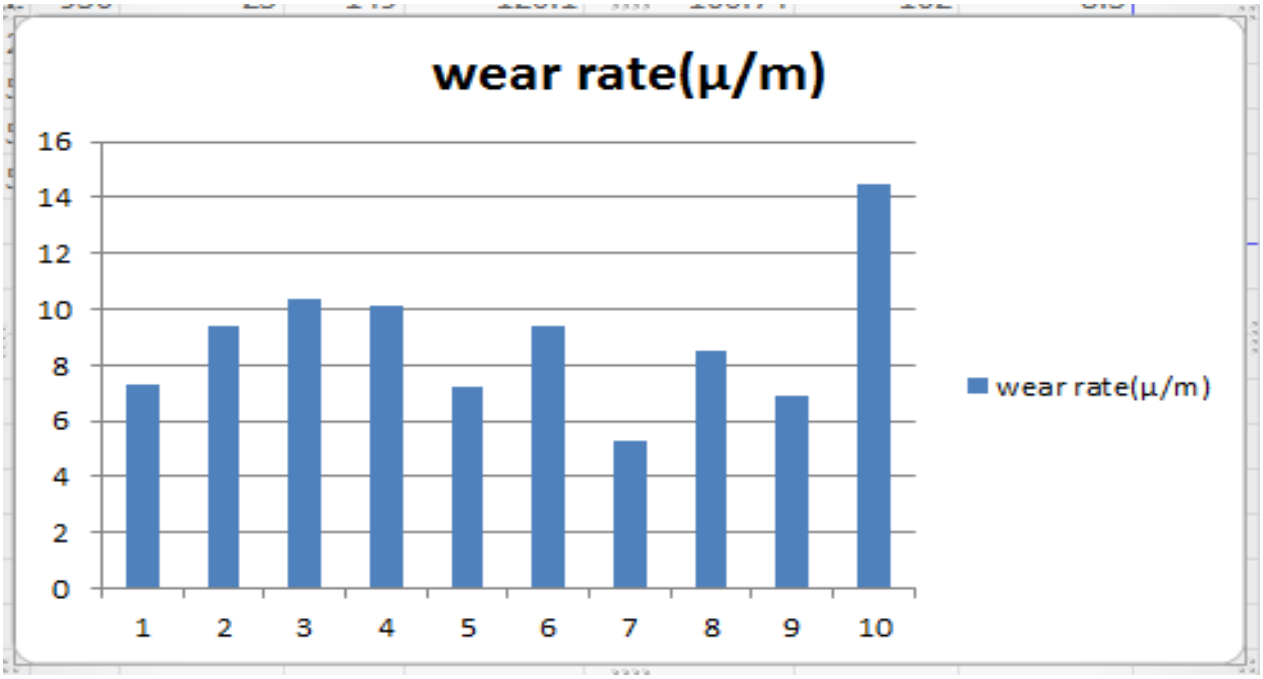

Figure 4.4.8 Wear rates for various specimens

4.5 Microstructure: Figure for various specimens from optical microscope and SEM:

Specimen 1:

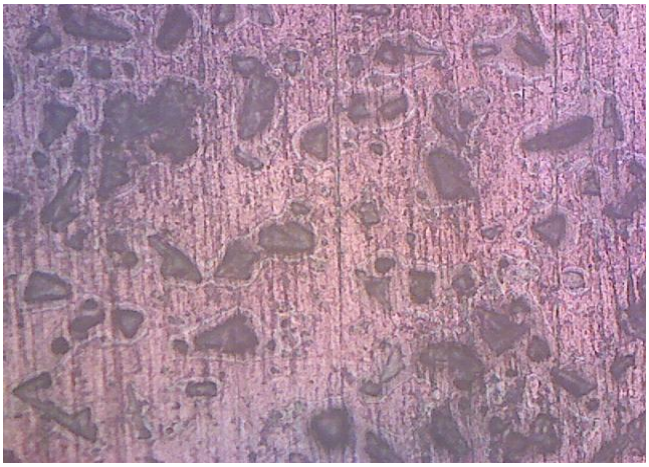

Specimen 2:

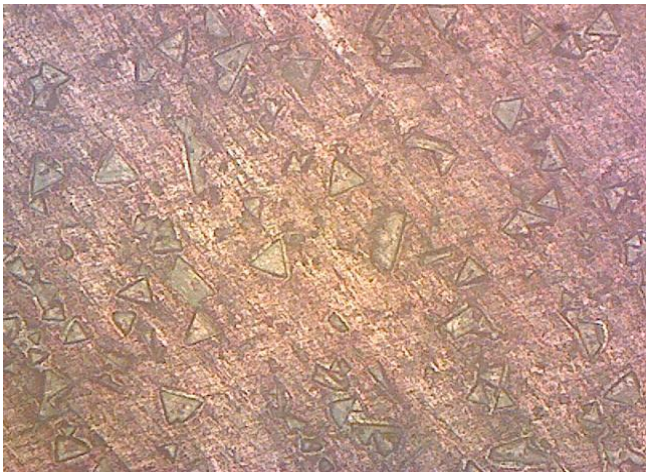

Specimen3:

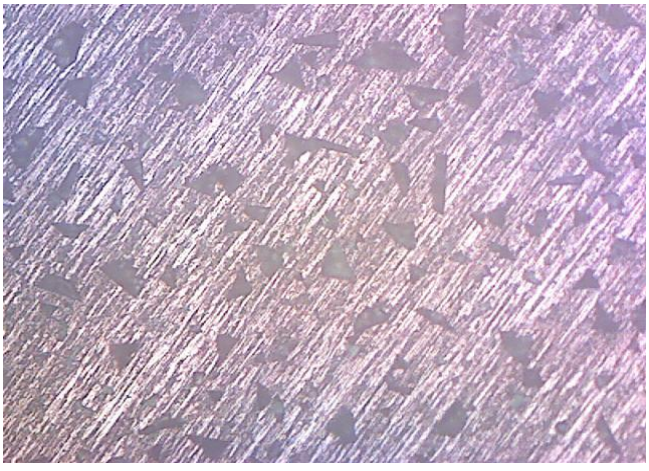

Specimen 4

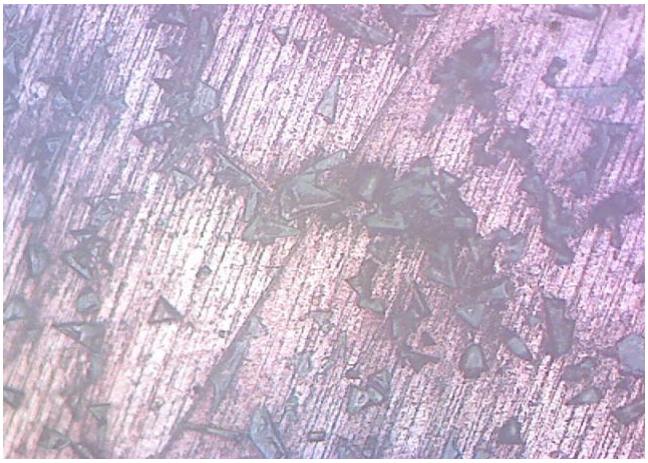

Specimen 5

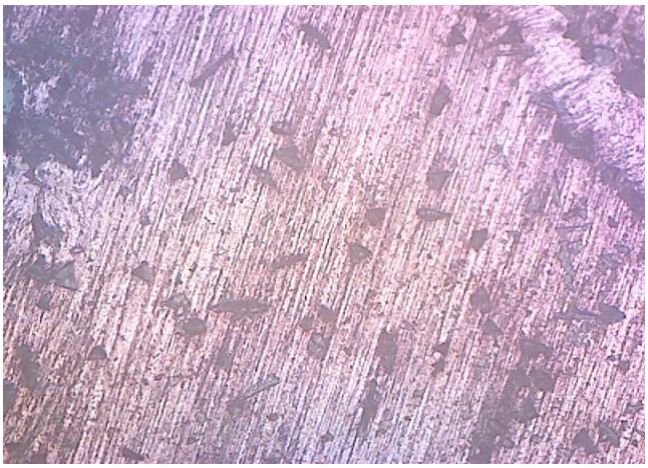

Specimen 6

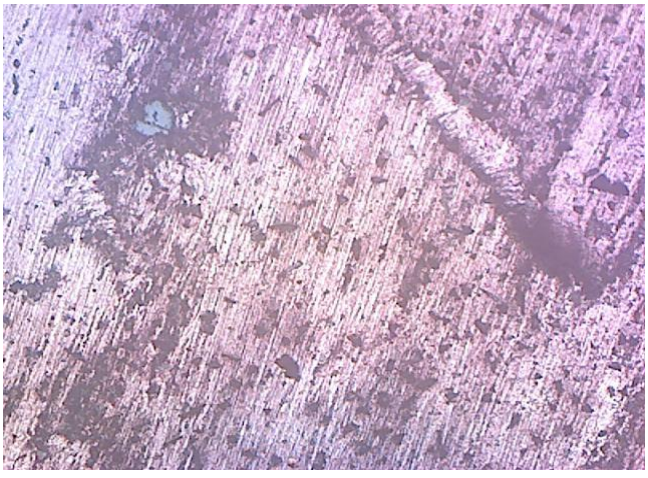

Specimen 7

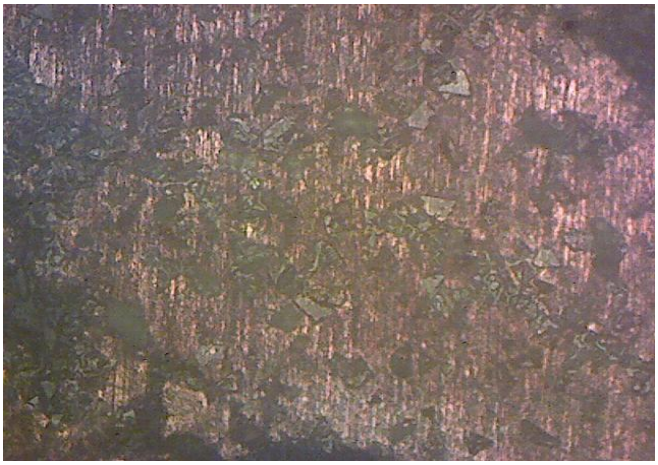

Specimen 8:

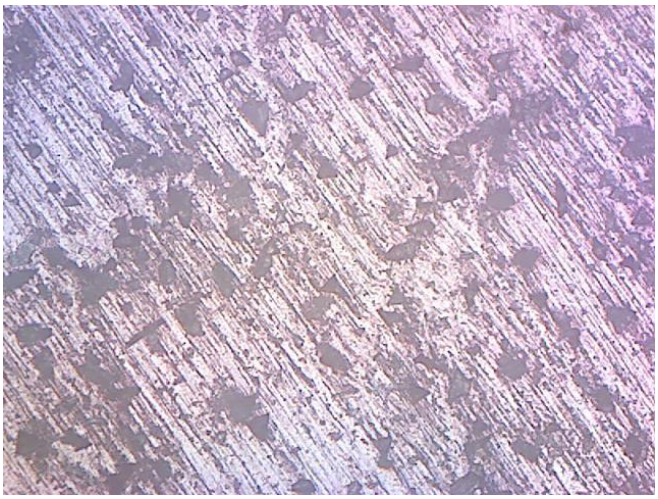

Specimen 9:

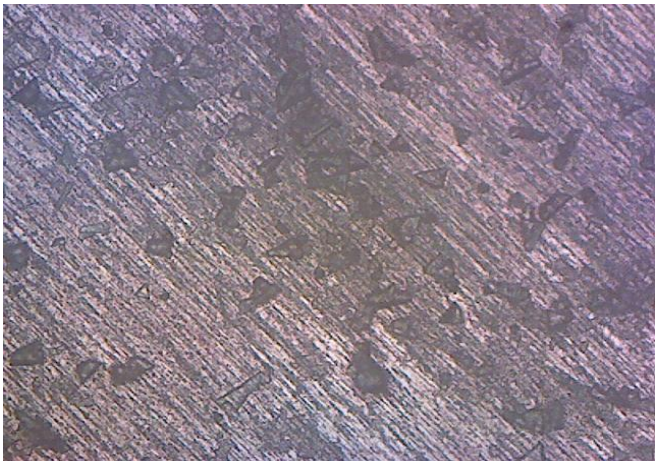

Specimen 10:

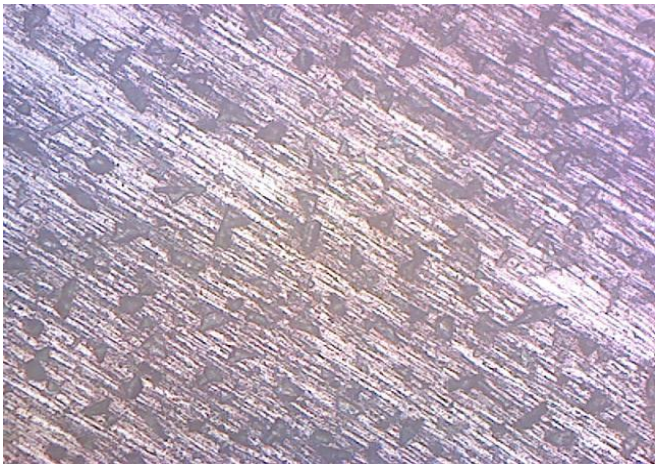

Some of the specimens revealed the clear picture of presence of graphite in the microstructure of surface composites .Specimen 4 showed the clear presence of graphite particles and in specimen 5 & 6 graphite particles are supposed to accumulated in a region. Grain boundaries aren't clearly visible.

Figures from SEM:

Specimen 1:

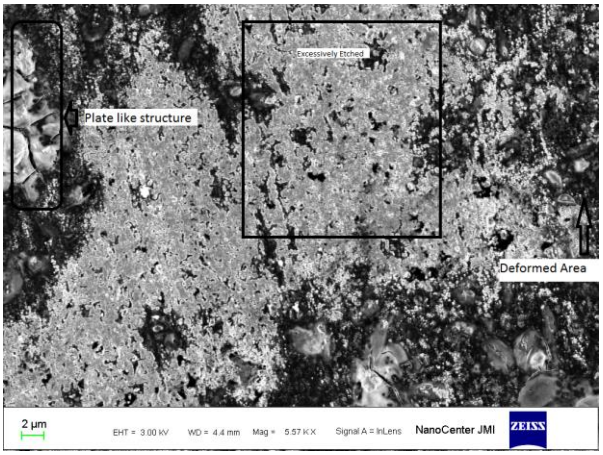

Specimen 2:

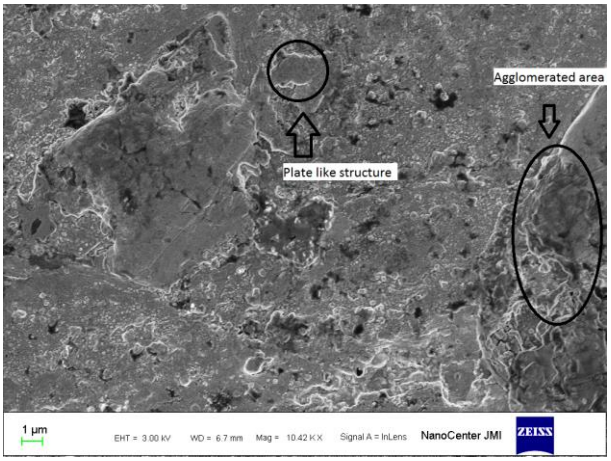

Specimen 3:

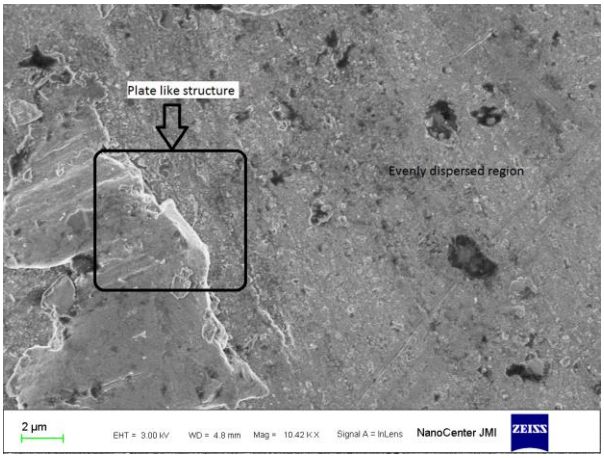

Specimen 4:

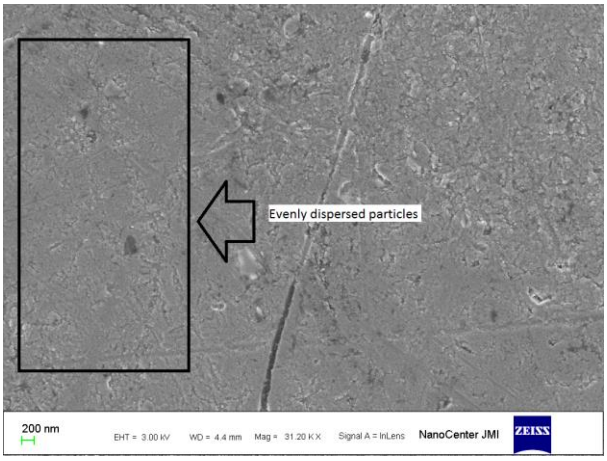

Specimen 5:

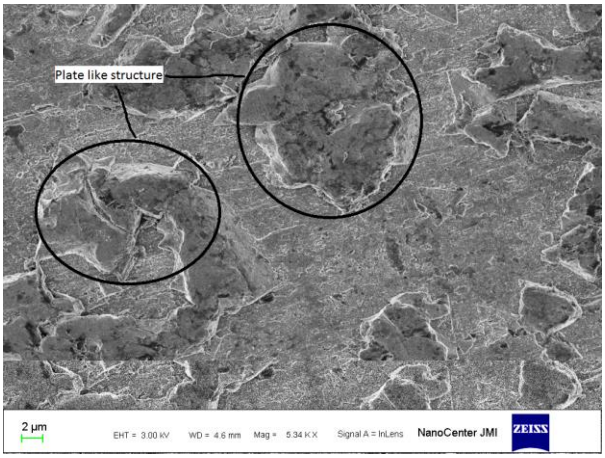

Specimen 6:

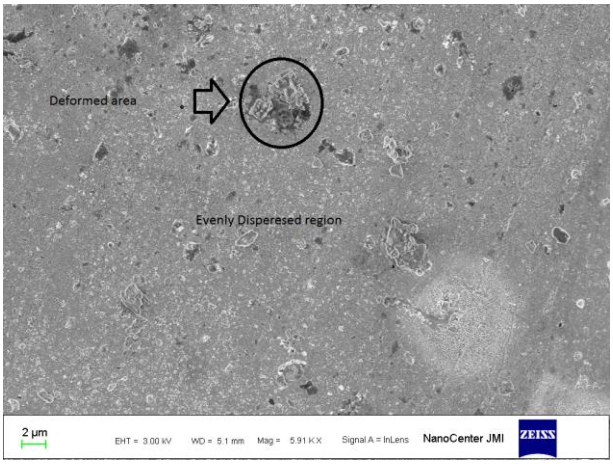

Specimen 7:

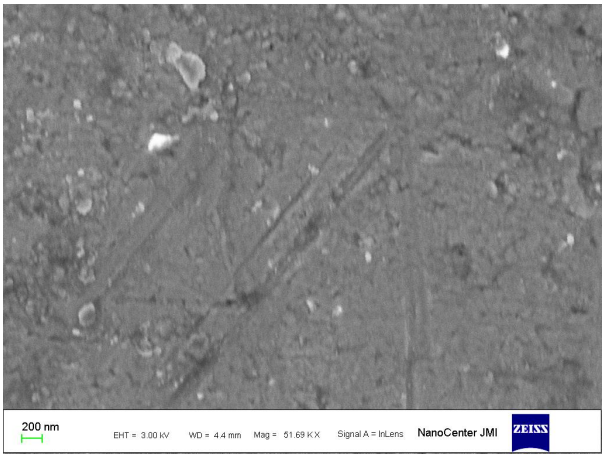

Specimen 8:

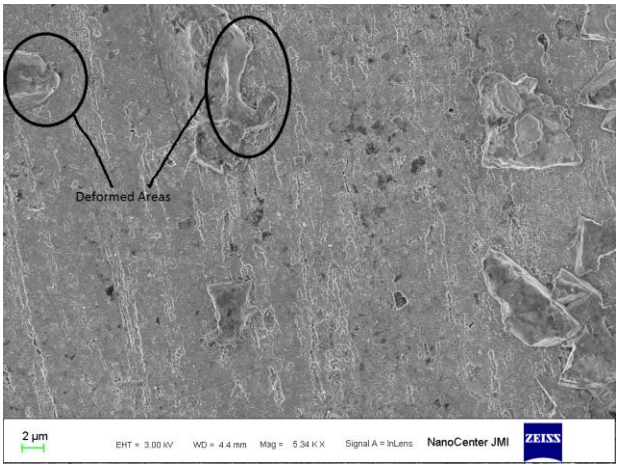

Specimen 9:

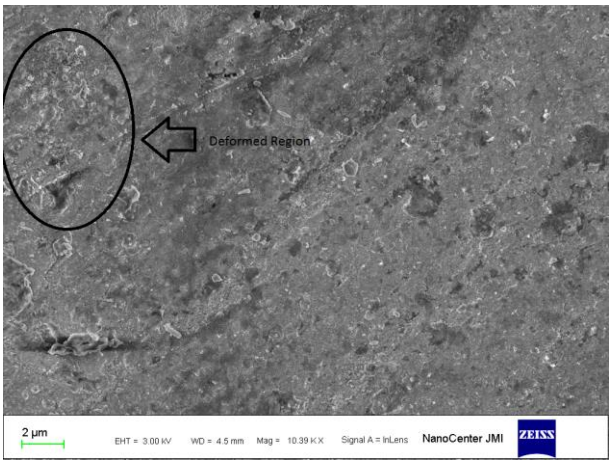

Specimen 10:

Above figure clearly showed the presence of graphite particles in the surface composites and has been shown in the figures. Although the graphite particles are not clearly visible in the figures via optical microscope. Only Specimen 1 shows images of excessively etched region. There is also a deformed regions and plate like structures also shown in the respective figures. Specimen Nos. 7 showed the perfect distribution of the graphite particles, which further ensures the reason for better wear resistance and lower coefficient of friction.

4.6 Graphs from Taguchi

Table 4.6

Taguchi process parameters table

Specimen Nos.	Tool tilt	Rotational Speed	Traverse Speed
6	1.5	**900**	**15**
8	**1.5**	**950**	**20**
7	**1.5**	**1000**	**25**
1	**2.0**	**900**	**20**
2	**2.0**	**950**	**25**
9	**2.0**	**1000**	**15**
3	**2.5**	**900**	**25**
4	**2.5**	**950**	**15**
5	**2.5**	**1000**	**20**

4.6.1 Signal-to-Noise:

In the Taguchi method, the term ‘signal’ represents the desirable value (mean) for the output characteristic and the term ‘noise’ represents the undesirable value (S.D.) for the output characteristic. Therefore, the S:N ratio is the ratio of the mean to the S.D. Taguchi uses the S:N ratio to measure the quality characteristic deviating from the desired value. [4]

Tensile Strength:

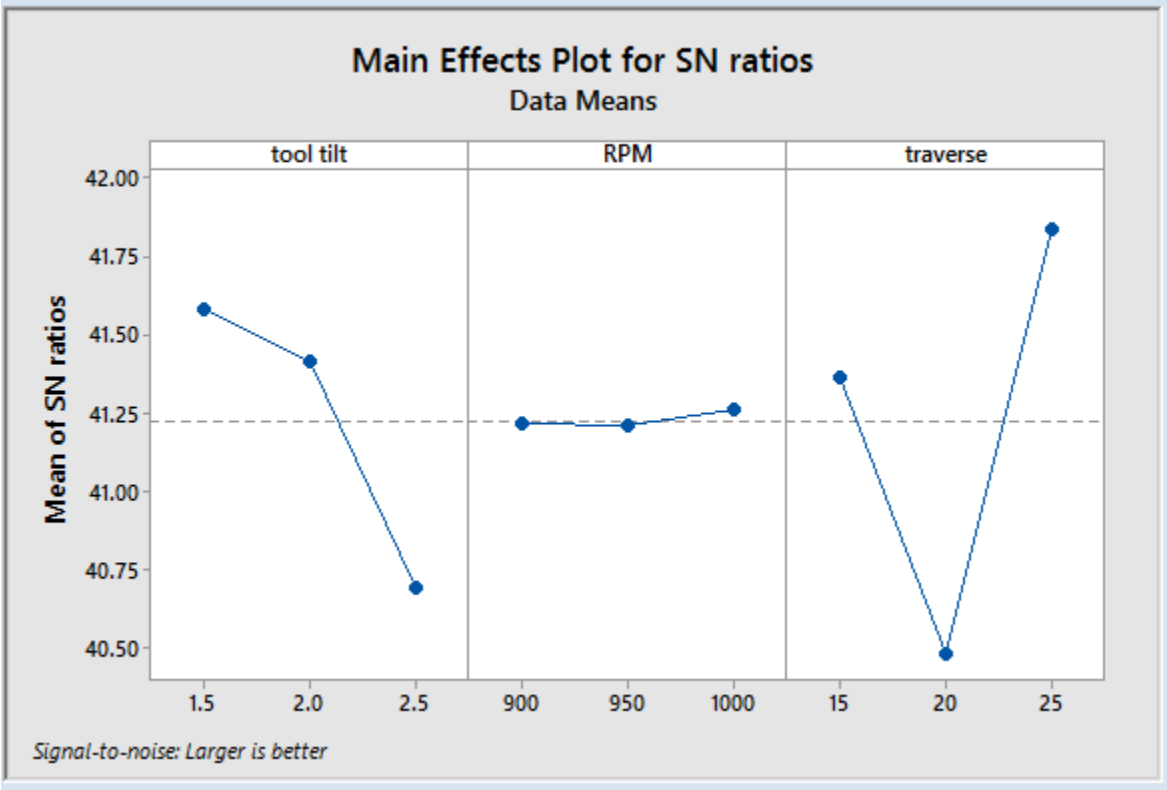

Figure 4.6.1 S/N ratio Plot for Tensile strength

Table 4.7 :S/N ratio for tensile

Symbol	Parameters	Mean S/N Ratio (dB)				
		Level 1	Level 2	Level 3	Max-min	Rank
A	Tool tilt	41.58	41.41	40.69	0.89	2
B	Rotational speed	41.21	41.21	41.26	0.05	3
C	Traverse Speed	41.37	40.48	41.84	1.36	1

Wear:

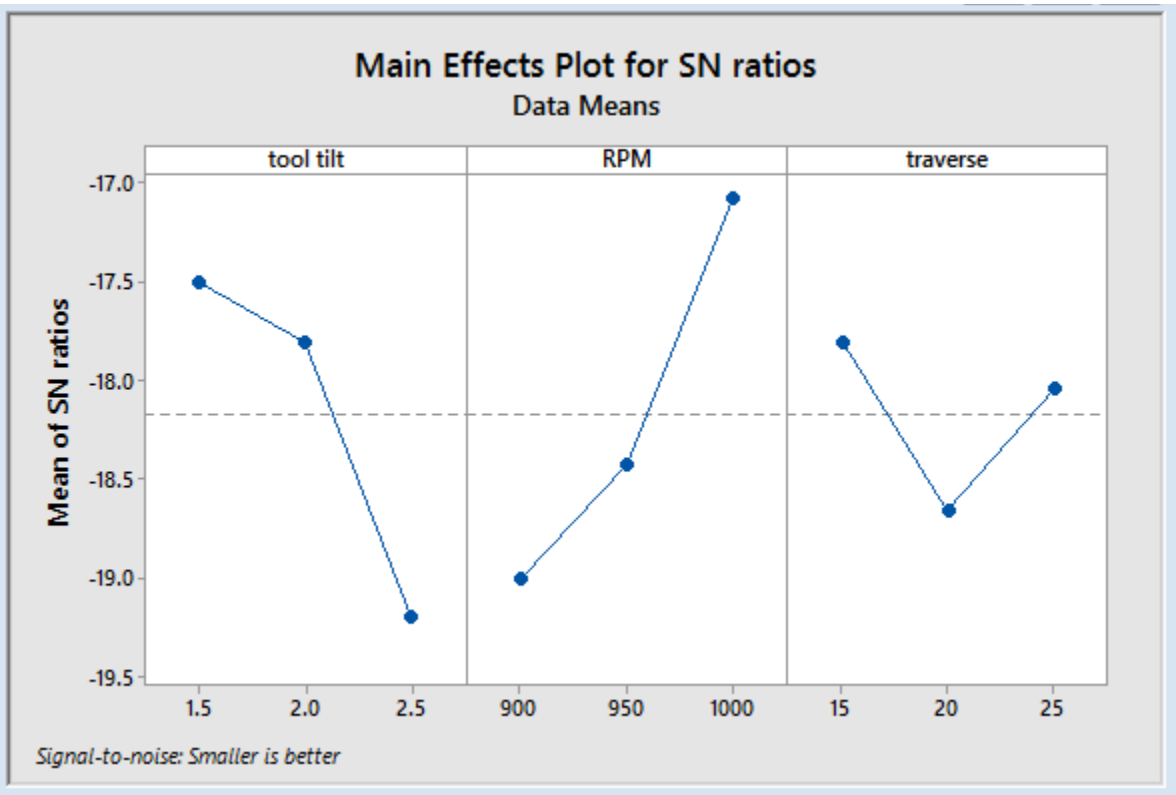

Figure 4.6.2 S/N ratio Plot for Wear

Table 4.8:S/N ratio for Wear

Symbol	Parameters	Mean S/N Ratio (dB)				
		Level 1	Level 2	Level 3	Min-max	Rank
A	Tool tilt	-17.50	-17.81	-19.20	1.70	2
B	Rotational speed	-19.00	-18.42	-17.08	1.93	1
C	Traverse Speed	-17.08	-18.66	-18.04	0.85	3

Microhardness:

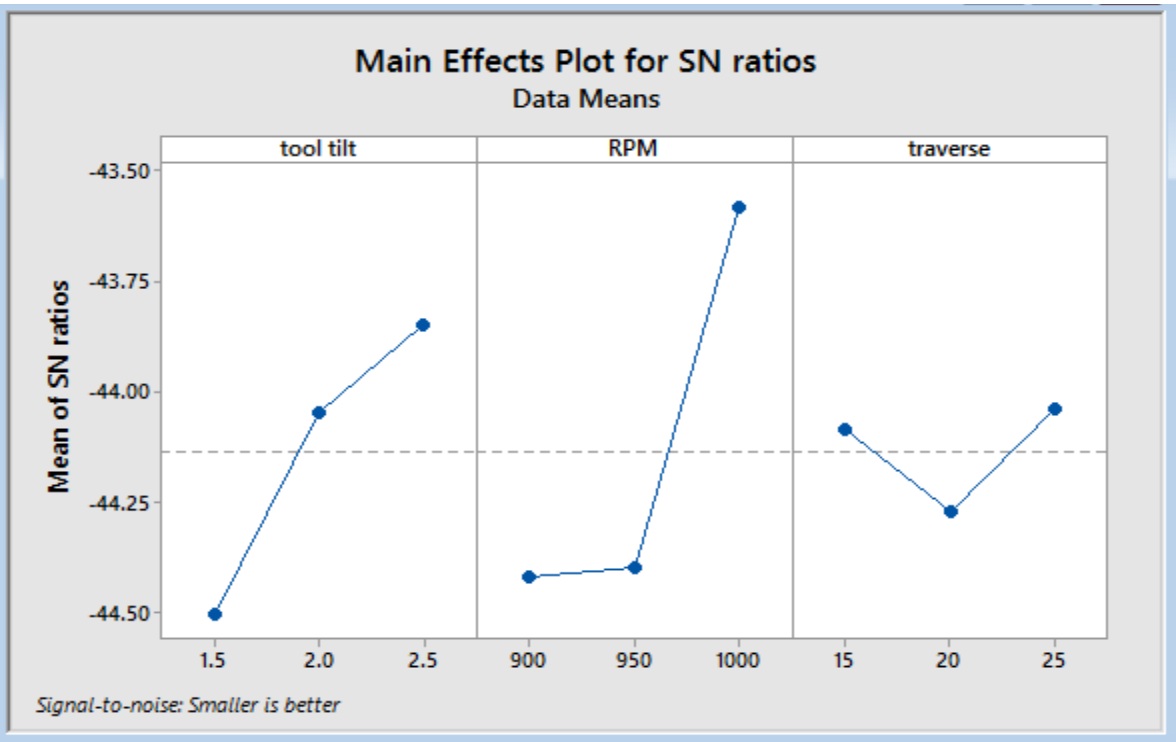

Figure 4.6.3 S/N ratio Plot for Microhardness

Table 4.9 :S/N ratio for microhardness

Symbol	Parameters	Mean S/N Ratio (dB)				
		Level 1	Level 2	Level 3	Min-max	Rank
A	Tool tilt	-44.50	-44.05	-43.85	0.66	2
B	Rotational speed	-44.42	-44.40	-43.58	0.84	1
C	Traverse Speed	-44.09	-44.27	-44.04	0.23	3

4.6.2 Mean:

The main effect plots are used to determine the optimal design conditions to obtain the optimal surface finish. According to this main effect plot, the optimal conditions for maximum tensile strength is A2B3C1 which is tool tilt at level 2 (2^0), Rotational speed at level 3 (1000 rpm) and

Traverse speed at level 1 (15mm/sec). The optimal conditions for minimum wear is A2B1C3 which is tool tilt at level 2 (2^0), Rotational speed at level 1(900rpm) and traverse speed at level 3 (25mm/min). The optimal conditions for maximum hardness is A2B1C3 which means tool tilt at level 2(2^0), Rotational speed at level 1(900rpm) and traverse speed at level 3 (25mm/min).

Tensile:

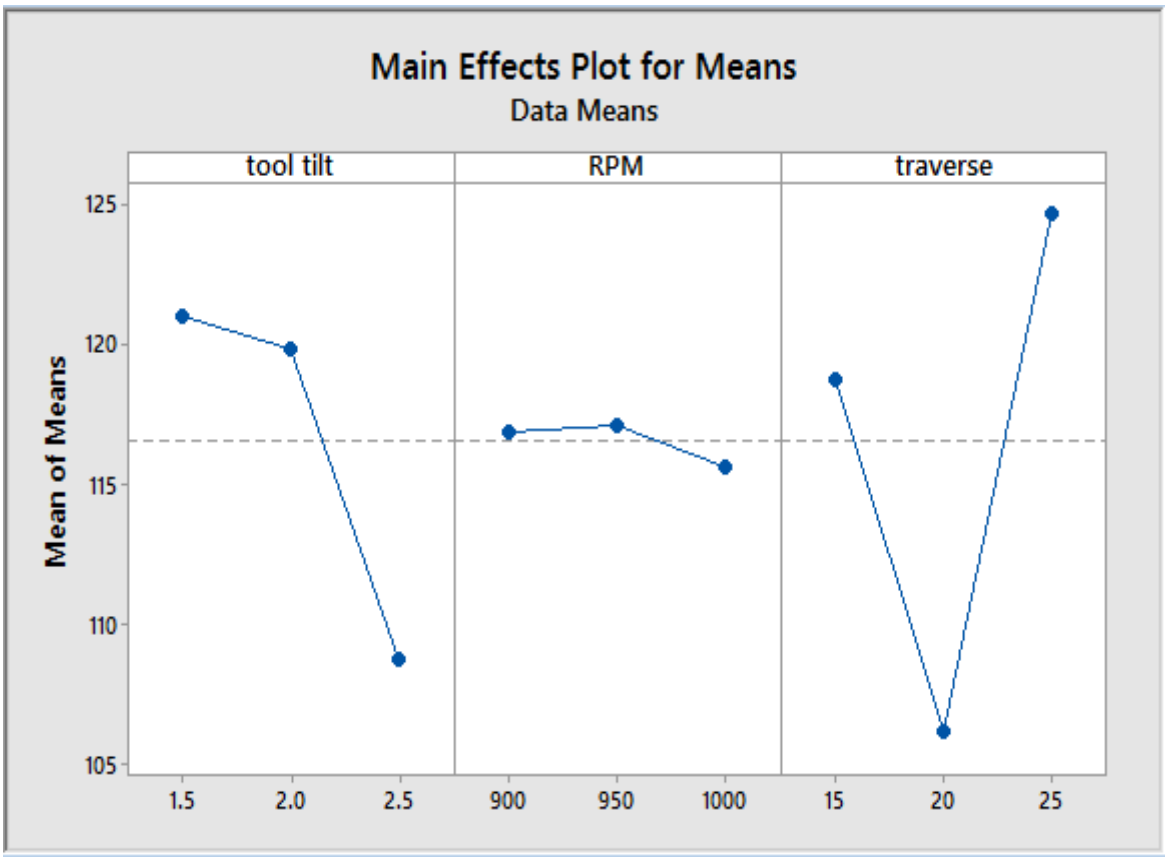

Figure 4.6.4 Means Plot for Tensile strength

Table 4.10: Means for tensile strength

Symbol	Parameters	Mean				
		Level 1	Level 2	Level 3	Min-max	Rank
A	Tool tilt	121.0	119.9	108.8	12.2	2
B	Rotational speed	116.9	117.1	115.7	1.4	3
C	Traverse Speed	118.8	106.2	124.7	18.5	1

Wear:

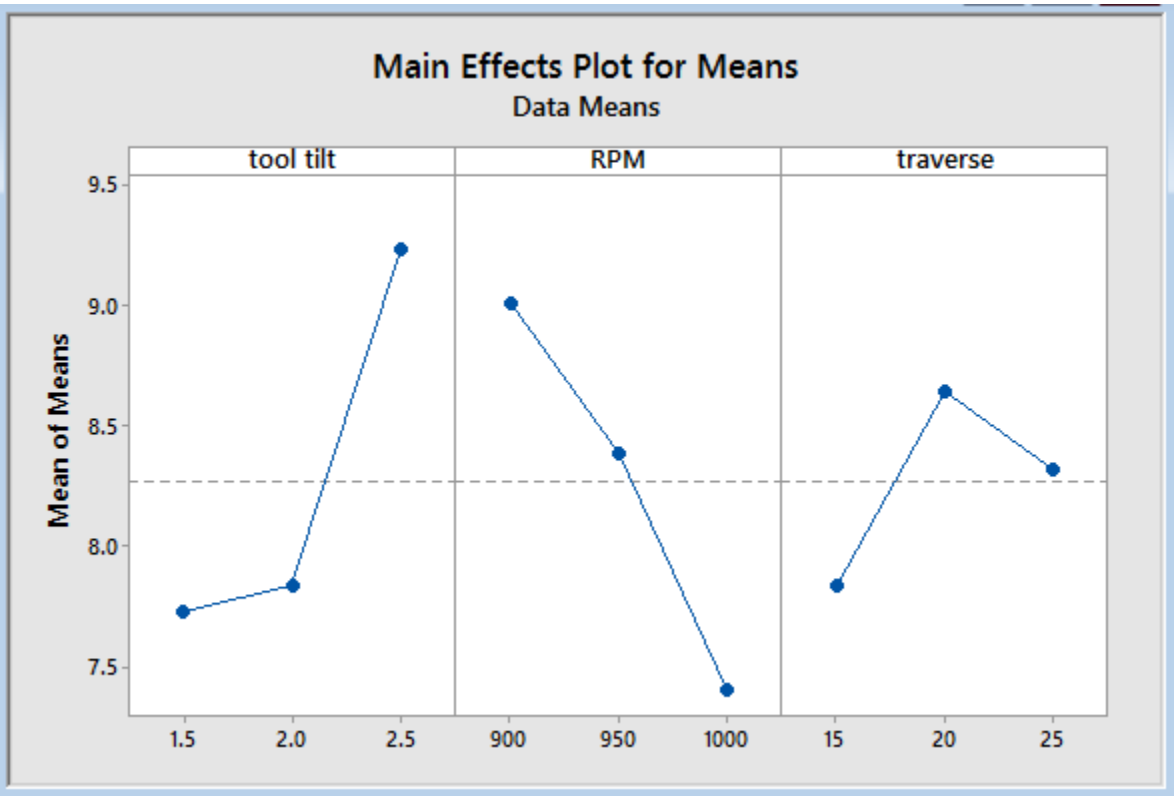

Figure 4.6.5 Means Plot for Wear

Table 4.11: Means for wear

Symbol	Parameters	Mean				
		Level 1	Level 2	Level 3	Min-max	Rank
A	Tool tilt	7.73	7.84	9.23	1.5	2
B	Rotational speed	9.01	8.38	7.40	1.6	1
C	Traverse Speed	7.84	8.64	8.31	0.80	3

Microhardness:

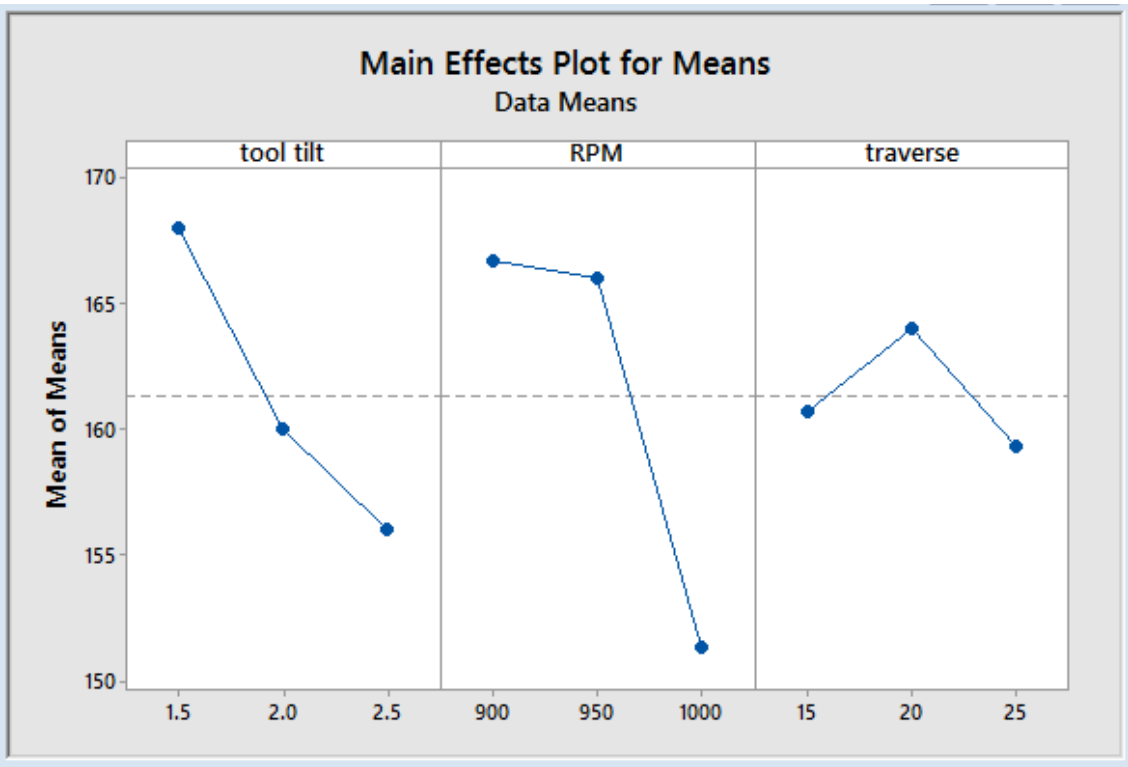

Figure 4.6.6 Means Plot for microhardness

Table 4.12: Means for microhardness

Symbol	Parameters	Mean				
		Level 1	Level 2	Level 3	Min-max	Rank
A	Tool tilt	168	160	156	12	2
B	Rotational speed	166.7	166.0	151.3	15.3	1
C	Traverse Speed	160.7	164.0	159.3	4.7	3

4.7 Graphs from Regression Analysis

4.7.1 Normal probability plot of Residuals for tensile strength, wear and hardness

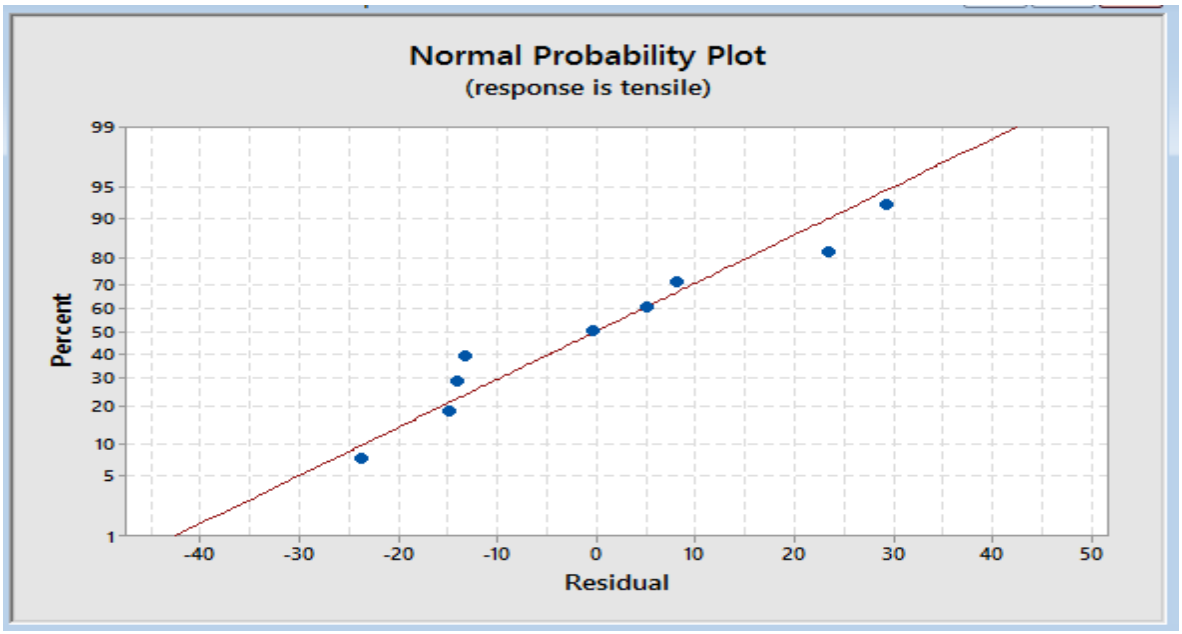

Figure 4.7.1

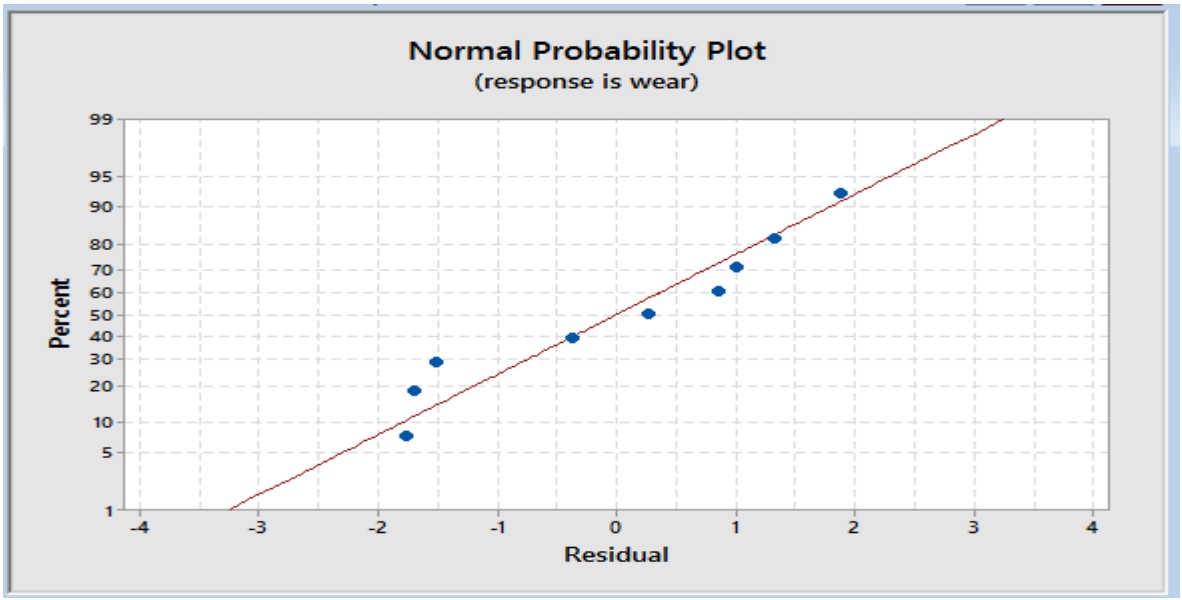

Figure 4.7.2

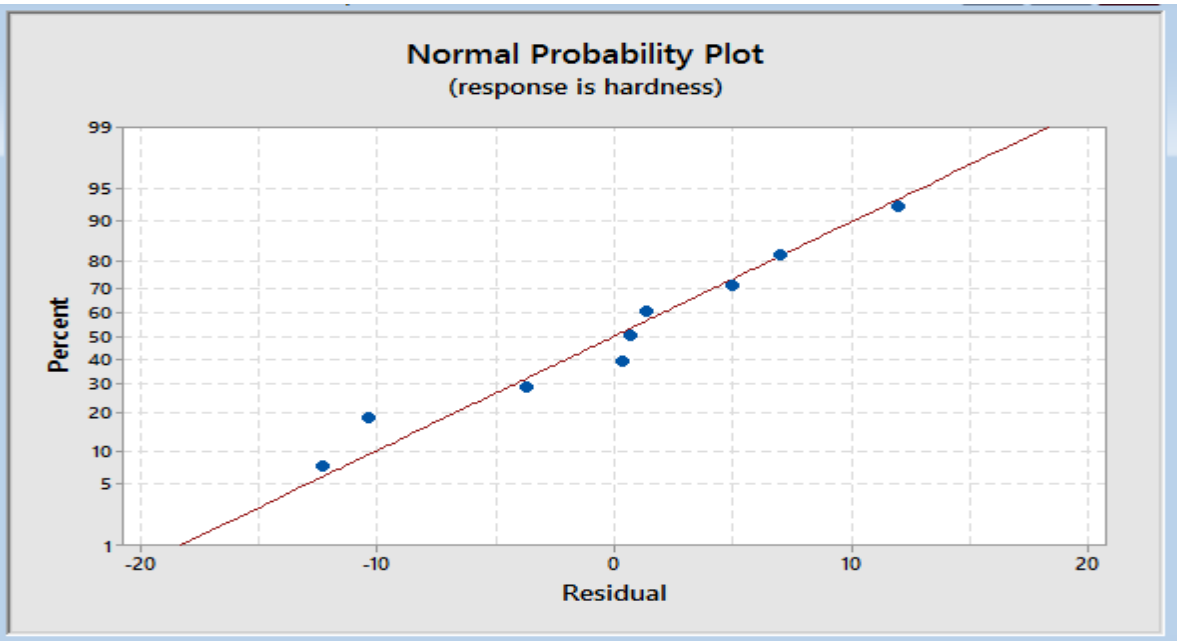

Figure 4.7.3

The points in this plot should generally form a straight line if the residuals are normally distributed. If the points on the plot depart from a straight line, the normality assumption may be invalid. As in this project work data have less than 50 observations, the plot may show bend in the tails even if the residuals are normally distributed. As the number of observations drops, the probability plot may show substantial difference and nonlinearity even if the residuals are normally distributed.

4.7.2 Residuals vs Fits for Tensile Strength ,wear and hardness

This plot should display a random pattern of residuals on both sides of 0. If a point lies distant from the majority of points, it may be an outlier. Also, there should not be any familiar patterns in the residual plot. The following may show error that is not random:

- a series of increasing or decreasing points
- a majority of positive residuals, or a majority of negative residuals
- patterns, such as increasing residuals with increasing fits

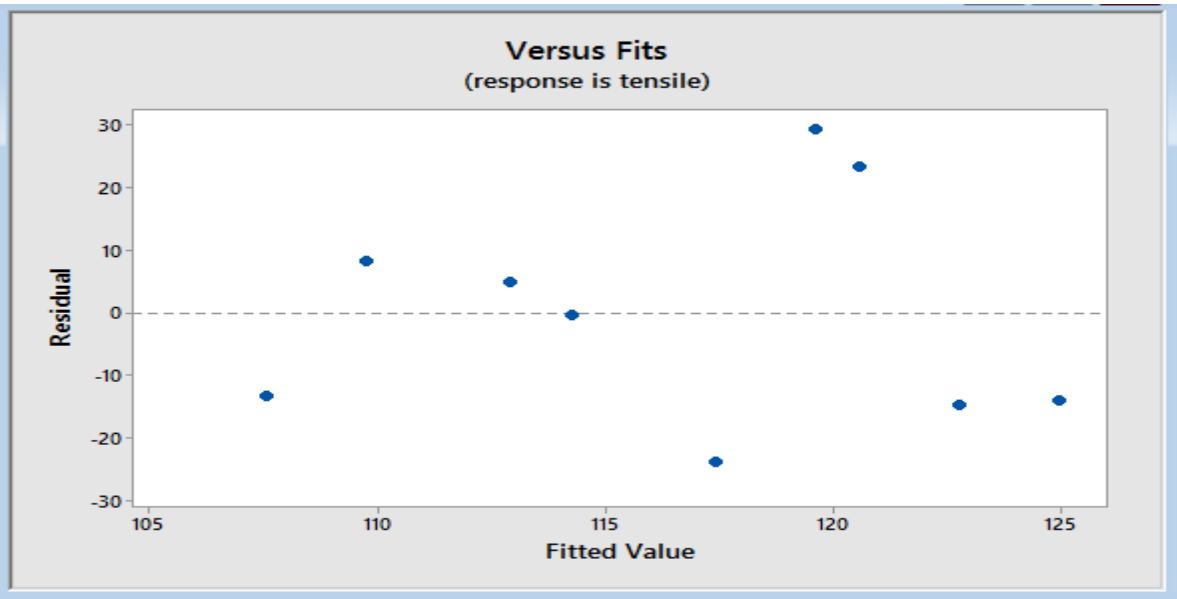

Figure 4.7.4

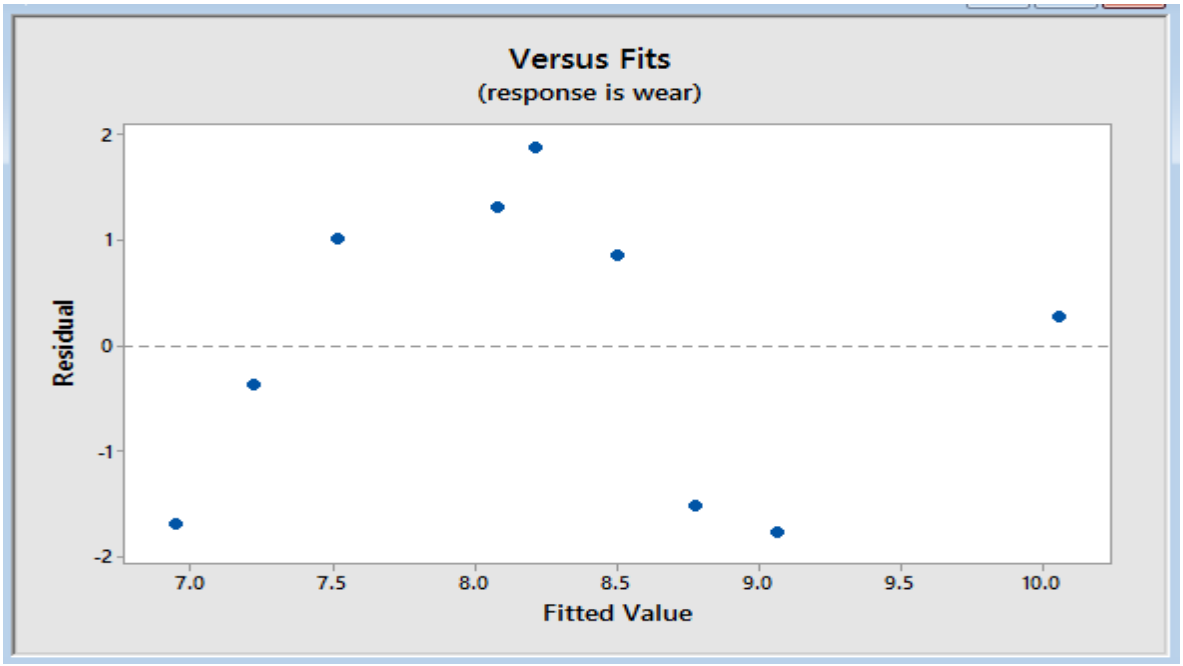

Figure 4.7.5

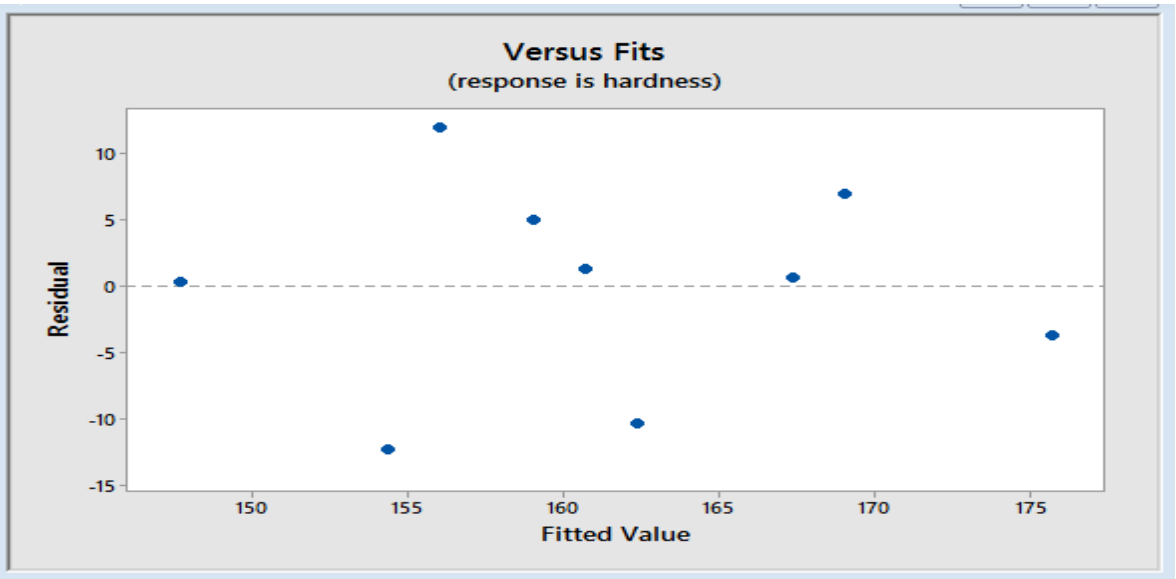

Figure 4.7.6

It can be concluded that all the values are within the control range, indicating that there is no obvious pattern and unusual structure.

4.7.3Residual Histogram for Tensile Strength wear and hardness

Long tails in the plot may indicate skewness in the data. If one or two bars are far from the others, those points may be outliers because the appearance of the histogram changes depending on the number of intervals used to group the data

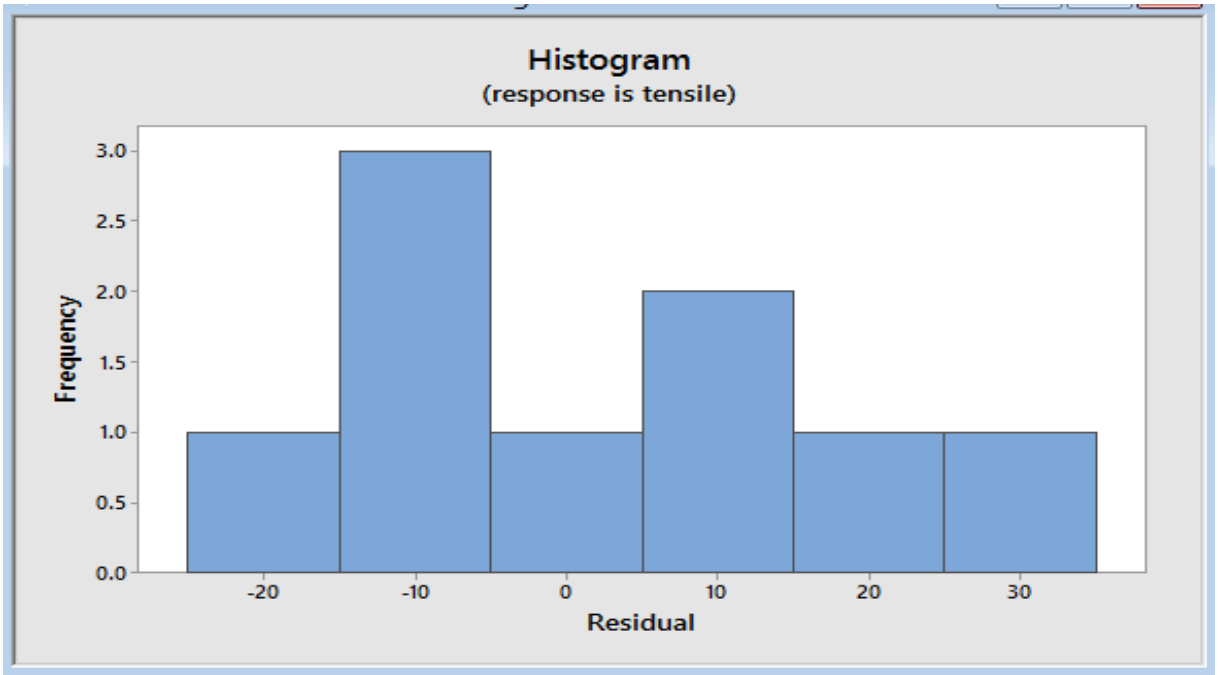

Figure 4.7.7

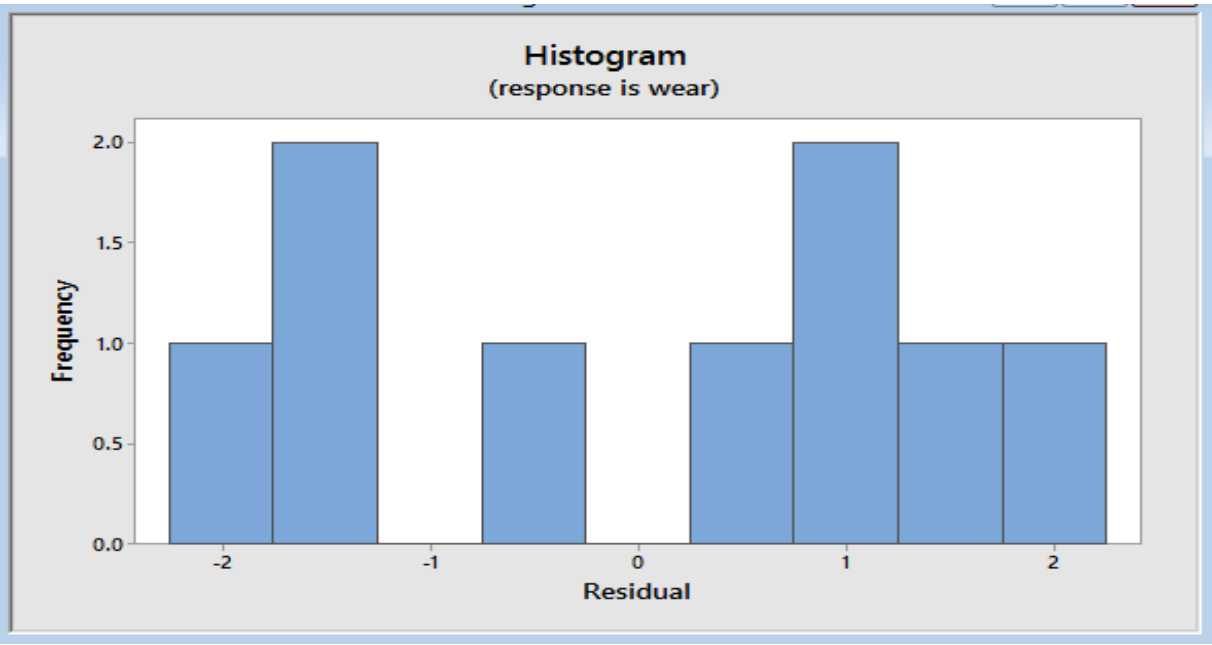

Figure 4.7.8

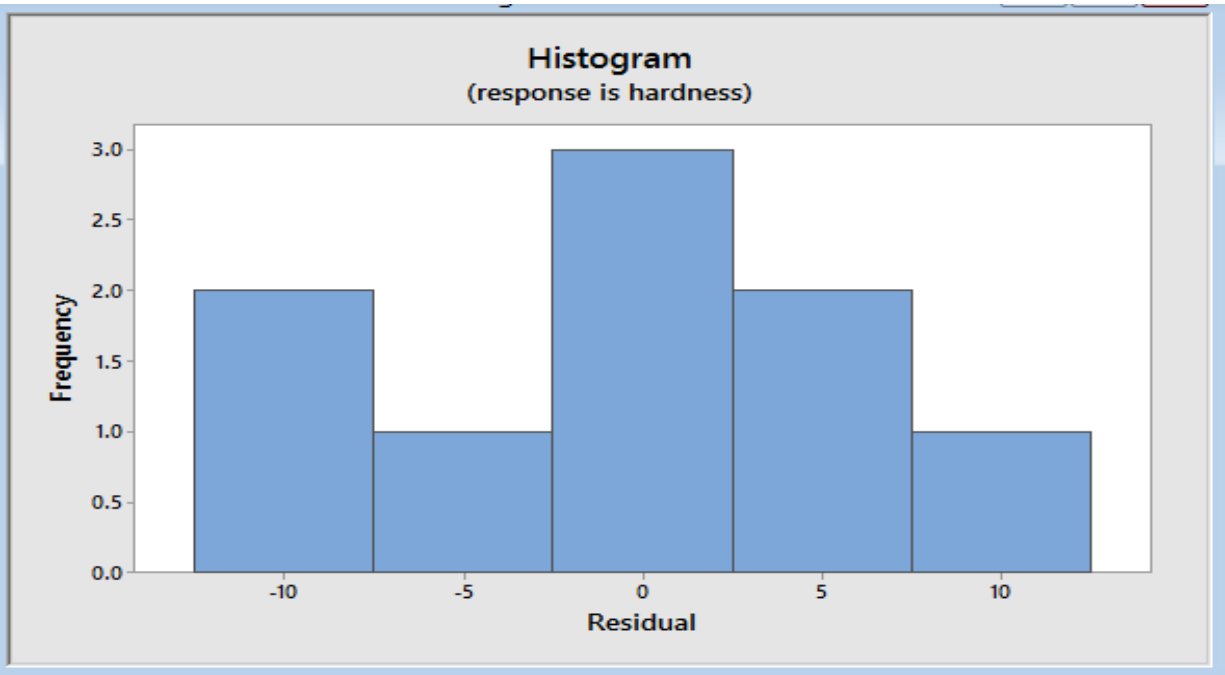

Figure 4.7.9

4.7.3 Residuals vs Order for tensile strength, wear and hardness

This is a plot of all residuals in the order that the data was collected and can be used to find non-random error, especially of time-related effects. A positive correlation is indicated by a clustering of residuals with the same sign and a negative correlation is indicated by rapid changes in the signs of consecutive residuals.

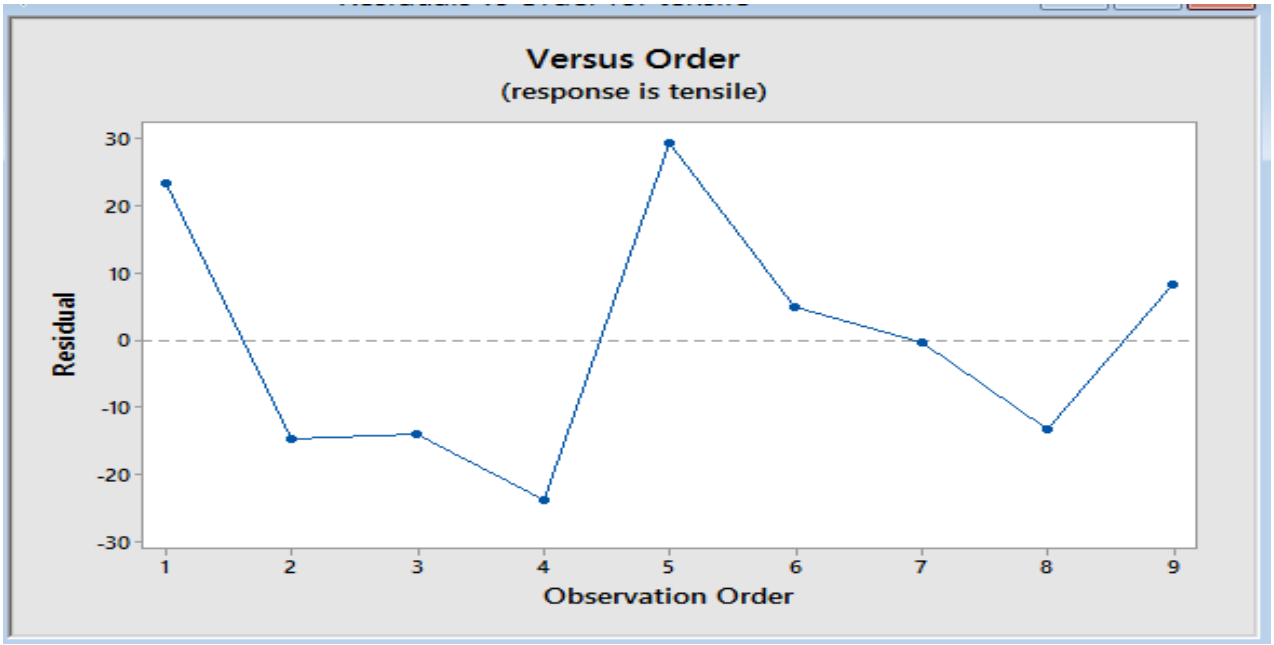

Figure 4.7.10

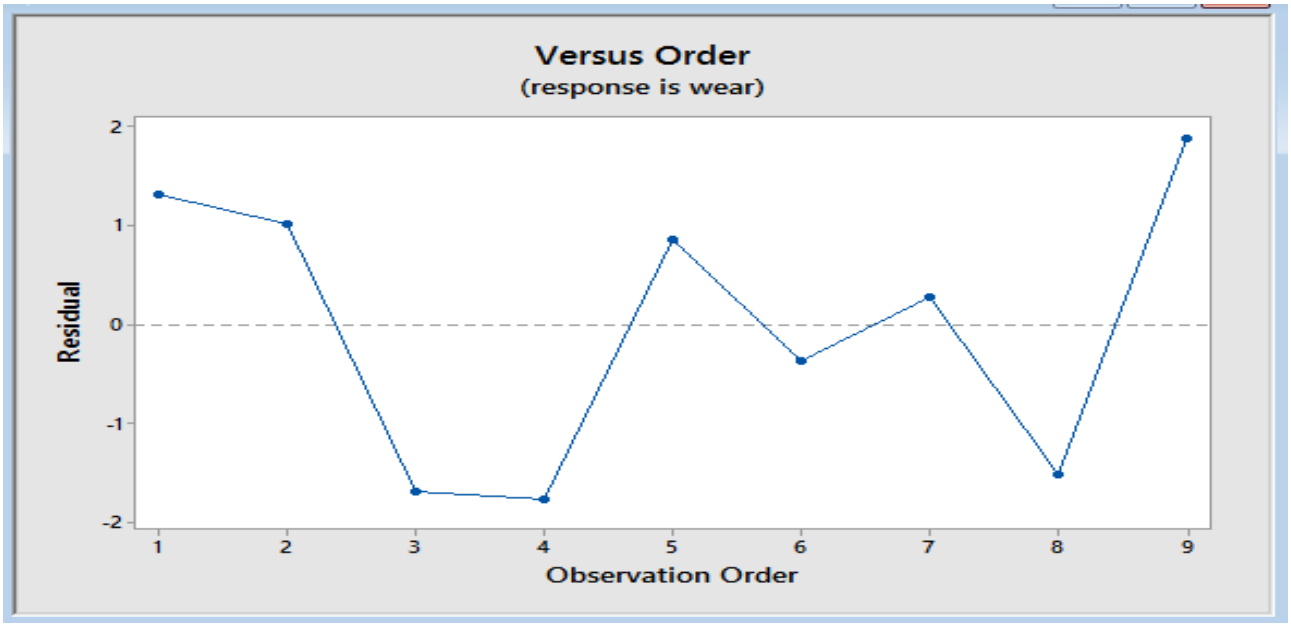

Figure 4.7.11

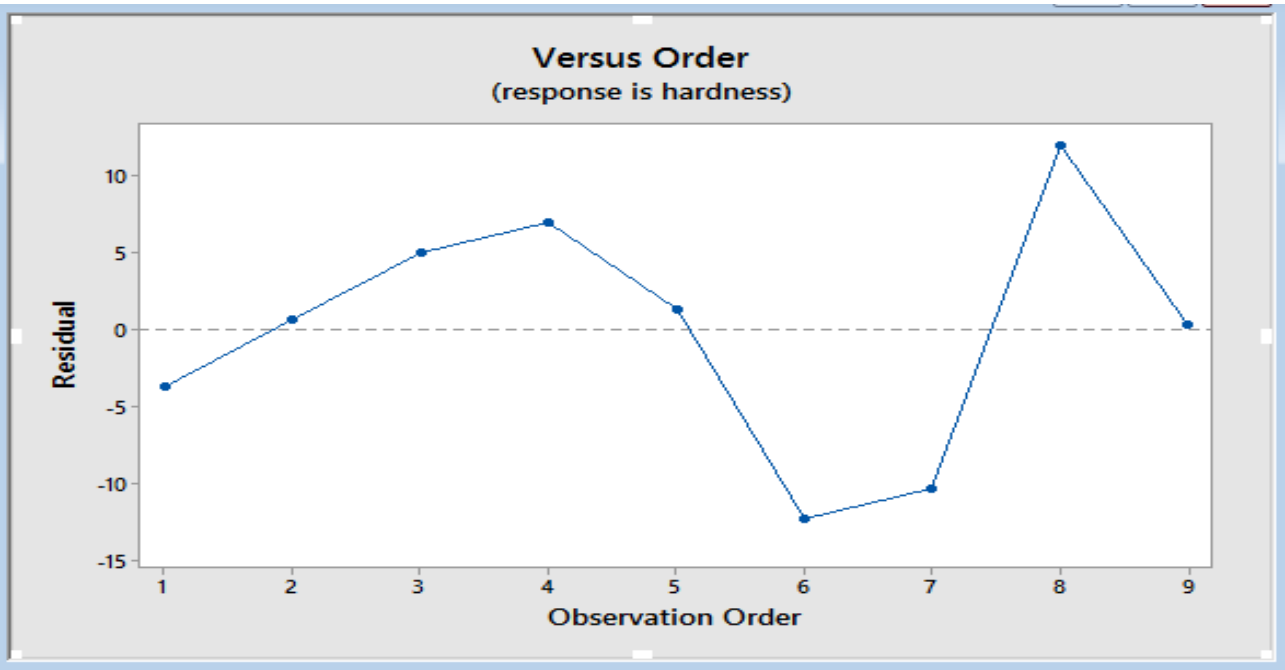

Figure 4.7.12

From graphs 4.7.1 to 4.7.12, it can be concluded that all the values are within the control range, indicating that there is no obvious pattern and unusual structure and also the residual analysis does not indicate any model inadequacy. Hence these values yield better results in future predictions.

4.7.4 Regression Equations:

Tensile strength = 144 - 12.2 tool tilt - 0.015 rpm + 0.59 traverse

Hardness = 333.7 - 12.00 tool tilt - 0.1533 rpm - 0.133 traverse

Wear = 19.5 + 1.50 tool tilt - 0.0160 rpm + 0.048 traverse

Regression tables:

Table 4.13

Tensile Strength

Tool tilt	RPM	Traverse speed	Actual	Calculated	FITS1	RESI1
1.5	900	15	144	121.05	120.589	23.4111
1.5	950	20	108	123.25	122.772	-14.7722
1.5	1000	25	111	125.45	124.956	-13.9556
1.5	900	20	93.6	117.9	117.422	-23.8222
1.5	950	25	149	120.1	119.606	29.3944
1.5	1000	15	118	113.45	112.939	5.0611
1.5	900	25	114	114.75	114.256	-0.2556
1.5	950	15	94.3	108.1	107.589	-13.2889
1.5	1000	20	118	110.3	109.772	8.2278

Table 4.14

Hardness (Hv)

Tool tilt	RPM	Traverse speed	Hv calculated	Hv actual	FITS2	RESI2
1.5	900	15	175.735	172	175.667	-3.6667
1.5	950	20	167.405	168	167.333	0.6667
1.5	1000	25	159.075	164	159.000	5.0000
1.5	900	20	169.07	176	169.000	7.0000
1.5	950	25	160.74	162	160.667	1.3333
1.5	1000	15	154.405	142	154.333	-12.3333
1.5	900	25	162.405	152	162.333	-10.3333
1.5	950	15	156.07	168	156.000	12.0000
1.5	1000	20	147.74	148	147.667	0.3333

Table 4.15

Wear rate

Tool tilt	RPM	Traverse speed	Wear actual	Wear calc.	FITS3	RESI3
1.5	900	15	7.3	8.07	8.0800	1.32000
1.5	950	20	9.36	7.51	7.5167	1.01333
1.5	1000	25	10.33	6.95	6.9533	-1.69333
1.5	900	20	10.1	9.06	9.0683	-1.76833
1.5	950	25	7.26	8.5	8.5050	0.85500
1.5	1000	15	9.4	7.22	7.2267	-0.36667
1.5	900	25	5.26	10.05	10.0567	0.27333
1.5	950	15	8.53	8.77	8.7783	-1.51833
1.5	1000	20	6.86	8.21	8.2150	1.88500

From Table 4.13, it can be concluded that the optimum combination process parameters for maximum strength is obtained at tool tilt of 2.0^0 , rotational speed of 1000rpm and traverse speed of 15mm/min.

From Table 4.14, it can be concluded that the optimum combination process parameters for maximum hardness is obtained at tool tilt of 2.0^0 , rotational speed of 900rpm and traverse speed of 25mm/min.

From Table 4.15, it can be concluded that the optimum combination process parameters for minimum wear rate is obtained at tool tilt of 2.0^0 , rotational speed of 900rpm and traverse speed of 25mm/min.

CHAPTER-5

CONCLUSIONS

Copper (99% pure) and graphite particles (approx. 6microns) surface composite was successfully synthesized using the novel method of FSP without any formation of defects. Effect of reinforcement particle on the microstructure, microhardness and wear properties of the surface composite produced was investigated by performing various tests on the sample.

Following were the major findings:

FSPed copper with graphite particle exhibited reduced hardness upto 142 Hv as compared to 180 Hv of the parent metal due to mixing of softer graphite particles in the matrix.

FSPed copper with graphite particle exhibited reduced tensile strength upto 93.6MPa of specimen 1 as compared to 300 MPa for the parent metal due to mixing of softer graphite particles in the matrix.

FSPed copper with graphite particle exhibited reduced wear rate upto 5.26 micron/m for specimen 7 as compared to 14.46 micron/m for the parent metal due to the sticking of graphite particles to sliding surfaces; therefore, sliding take place within interior layers of graphite particles which consequently leads to decrease in value of friction coefficient upto 0.168 from 0.49 for parent metal.

The rotational speed is the major parameters among the three controllable factors (tool tilt, rotational speed and traverse speed) that influence the wear resistance and hardness of the surface composites prepared from FSP.

The traverse speed is the major parameters among the three controllable factors (tool tilt, rotational speed and traverse speed) that influence the tensile strength of the surface composites prepared from FSP.

The optimum combination process parameters for minimum wear rate and hardness/micro hardness is obtained at tool tilt of 2.0^0, rotational speed of 900rpm and traverse speed of 25mm/min.

The optimum combination process parameters for maximum strength is obtained at tool tilt of 2.0^0, rotational speed of 1000rpm and traverse speed of 15mm/min.

References:

1.Friction Stir Processing of Aluminum alloys for Defense Applications V. Jeganathan Arulmoni, R. S. Mishra

2. Effect of Process Parameters on Friction Stir Processed Copper and Enhancement of Mechanical Properties of the Composite Material: A Review on Green Process Technology V.Jeganathan Arulmoni, Ranganath M S, R S Mishra.

3. Development of high strength, high conductivity copper by friction stir processing K. Surekha , A. Els-Botes.

4. Developments of nanocrystalline structure in Cu during friction stir processing (FSP) Jian-Qing Sua, T.W. Nelson, T.R. McNelley, R.S. Mishra.

5. H. Khodaverdizadeh , A. Mahmoudi , A. Heidarzadeh , E. Nazari, [2012] Effect of friction stir welding (FSW) parameters on strain hardening behavior of pure copper joints.

6. Heidarzadeh, T. Saeid, [2013] Prediction of mechanical properties in friction stir welds of pure copper,Materials and Design .

7. Characterization of oxide dispersion strengthened copper based materials developed by friction stir processing M.-N. Avettand-Fènoël ,A. Simar , R. Shabadi , R. Taillard , B. de Meester .

8. Hamed Pashazadeh , Jamal Teimournezhad , Abolfazl Masoumi, [2013] Numerical investigation on the mechanical, thermal, metallurgical and material flow characteristics in friction stir welding of copper sheets with experimental verification.

9. Prediction of mechanical and wear properties of copper surface composites fabricated using friction stir processing R. Sathiskumar , N. Murugan , I. Dinaharan , S.J. Vijay .

10. I. Galvao, A. Loureiro and D. M. Rodrigues, [2012] Influence of process parameters on the mechanical enhancement of copper-DHP by FSP.

11. Friction stir forming to fabricate copper–tungsten composite by Yogita Ahujaa, Raafat Ibrahima, Anna Paradowskab, Daniel RileybaMonash

12. Flow visualization and estimation of strain and strain-rate during friction stir process S. Mukherjee, A.K. Ghosh.

13. Masoud Jabbari, [2014] Elucidating of rotation speed in friction stir welding of pure copper.

14. Mohsen Barmouz, Mohammad Kazem Besharati Givi, [2011] Fabrication of in situ Cu/SiC composites using multi-pass friction stir processing: Evaluation of microstructural, porosity, mechanical and electrical behavior.

15. Enhanced strength and ductility of friction stir processed Cu–Al alloys with abundant twin boundaries P. Xue, B.L. Xiao and Z.Y. Ma

16. P. Xue, B.L. Xiao, Z.Y. Ma, [2013] Achieving Large-area Bulk Ultrafine Grained Cu via Submerged Multiple-pass Friction Stir Processing, J. Mater. Sci. Technol.

17. Article Effect of ceramic particulate type on microstructure and properties of copper matrix composites synthesized by friction stir processing Issac Dinaharan, Ramasamy Sathiskumar, Nadarajan Murugan

18. Influence of rotational speed on the formation of friction stir processed zone in pure copper at low-heat input conditions S. Cartigueyen, K. Mahadevan.

19. R. Sathiskumar, N. Murugan, I. Dinaharan, S.J. Vijay, [2013] Characterization of boron carbide particulate reinforced in situ copper surface composites synthesized using friction stir processing.

20. S. Mukherjee, A.K. Ghosh, [2011] Friction stir processing of direct metal deposited copper–nickel 70/30.

21. Effect of friction stir processing parameters on the microstructural and electrical properties of copper R. M. Leal1,2 & I. Galvão1 & A. Loureiro1 & D. M. Rodrigues.

22. J.J. Shen, H.J. Liu , F. Cui, [2010] Effect of welding speed on microstructure and mechanical properties of friction stir welded copper, Materials and Design .

23. Effect of Single and Multiple-Pass Friction Stir Processing on Microstructure, Hardness and Tensile Properties of a 99.99% Cu with Carbon Nano Tubes by V. Jeganathan Arulmoni, R. S. Mishra.

24. Effect of Process Parameters on Friction Stir Processed Copper and Enhancement of Mechanical Properties of the Composite Material by V. Jeganathan Arulmoni, Ranganath M. S., R. S. Mishra.

25. R. S. Mishra and Z. Y. Ma, "Friction stir welding and processing," Materials Science and Engineering R: Reports, vol. 50, 2005.

26. R. Bauri, D. Yadav, and G. Suhas, "Effect of friction stir processing (FSP) on microstructure and properties of Al-TiC in situ composite," Materials Science and Engineering A, vol. 528, pp. 4732-4739, 2011.

27. Surface composites by friction stir processing: A review Vipin Sharma, Ujjwal Prakash, B.V. Manoj Kumar

28. Assessment of microstructure and wear behavior of aluminum nitrate reinforced surface composite layers synthesized using friction stir processing on copper substrate S. Saravanakumar , S. Gopalakrishnan , I. Dinaharan , K. Kalaiselvan .

29. Prediction of mechanical and wear properties of copper surface composites fabricated using friction stir processing R. Sathiskumar , N. Murugan , I. Dinaharan , S.J. Vijay.

30. Friction stir selective alloying G.M. Karthik, G.D. Janaki Ram, Ravi Sankar Kottada.

31. M. D. Fuller, S. Swaminathan, A. P. Zhilyaev, and T. R. McNelley, "Microstructural transformations and mechanical properties of cast NiAl bronze: Effects of fusion welding and friction stir processing," Materials Science and Engineering A, vol. 463, pp. 128-137, 2007.

32. K. Oh-Ishi and T. R. McNelley, "Microstructural modification of as-cast NiAl bronze by friction stir processing," Metallurgical and Materials Transactions A: Physical Metallurgy and Materials Science, vol. 35 A, pp. 2951-2961, 2004.

33. Effect of ceramic particulate type on microstructure and properties of copper matrix composites synthesized by friction stir processing *Issac Dinaharana, Ramasamy Sathiskumarb, Nadarajan Muruganb.*

34. Role of Friction Stir Processing on Copper and Copper based Particle Reinforced Composites S.Cartigueyen and K.Mahadevan

35. Microstructure and wear characterization of rice husk ash reinforced copper matrix composites prepared using friction stir processing I. Dinaharan , K. Kalaiselvan , E.T. Akinlabi , J. Paulo Davim.

36. P. Cavaliere, "Mechanical properties of Friction Stir Processed 2618/Al2O3 metal matrixcomposite," Composites Part A: Applied Science and Manufacturing, vol. 36, pp. 1657-1665, 2005.

37. K. J. Hodder, H. Izadi, A. G. McDonald, and A. P. Gerlich, "Fabrication of aluminum–alumina metal matrix composites via cold gas dynamic spraying at low pressure followed by friction stir processing," Materials Science and Engineering: A, vol. 556, pp. 114-121, 2012.

38. Y. Morisada, H. Fujii, T. Mizuno, G. Abe, T. Nagaoka, and M. Fukusumi, "Modification of thermally sprayed cemented carbide layer by friction stir processing," Surface and Coatings Technology, vol. 204, pp. 2459-2464, 2010.

39. Y. Morisada, H. Fujii, T. Nagaoka, and M. Fukusumi, "MWCNTs/AZ31 surface composites fabricated by friction stir processing," Materials Science and Engineering A, vol. 419, pp. 344-348, 2006.

40. C. J. Lee, J. C. Huang, and P. J. Hsieh, "Mg based nano-composites fabricated by friction stir processing," Scripta Materialia, vol. 54, pp. 1415-1420, 2006.

41. R. S. Mishra, Z. Y. Ma, and I. Charit, "Friction stir processing: A novel technique for fabrication of surface composite," Materials Science and Engineering A, vol. 341, pp. 307-310, 2003.

42. A. Shafiei-Zarghani, S. F. Kashani-Bozorg, and A. Zarei-Hanzaki, "Microstructures and mechanical properties of Al/Al2O3 surface nano-composite layer produced by friction stir processing," Materials Science and Engineering A, vol. 500, pp. 84-91, 2009.

43 M. Yang, C. Xu, C. Wu, K. C. Lin, Y. J. Chao, and L. An, "Fabrication of AA6061/Al2O3 nano ceramic particle reinforced composite coating by using friction stir processing," Journal of Materials Science, vol. 45, pp. 4431-4438, 2010.

44 M. Dixit, J. W. Newkirk, and R. S. Mishra, "Properties of friction stir-processed Al 1100-NiTi composite," Scripta Materialia, vol. 56, pp. 541-544, 2007.